The LSP Stability and New Higgs Signals at the LHC

Pavel Fileviez Pérez,[*] Sogee Spinner,[†] and Maike K. Trenkel[‡]

Phenomenology Institute, Department of Physics,

University of Wisconsin-Madison, 1150 University Avenue, Madison, Wisconsin 53706, USA

(Dated: January 18, 2013)

The fate of R-parity in the context of the minimal supersymmetric standard model is a central issue which has profound implications for particle physics and cosmology. In this article we discuss the possibility of testing the mechanism responsible for the stability of the lightest supersymmetric particle at the Large Hadron Collider (LHC). The simplest theoretical framework where R-parity conservation can be explained dynamically allows for two types of B-L models. In the first scenario the new Higgses decay mainly into two right-handed neutrinos giving rise to exotic lepton number violating signals together with displaced vertices. In the second model one could have peculiar channels with multileptons and/or multiphotons in the final state. In both cases, the local B-L gauge symmetry is broken at the TeV scale and the discovery of the new Higgs bosons may be possible at the LHC. We investigate in detail the production mechanisms for the Higgs bosons relevant for the LHC and the key decays which would shed light on how R-parity is conserved. These results may help to understand the link between the cold dark matter of the universe and the missing energy that could be observed at the LHC if supersymmetry is realized in nature.

---

[*]Electronic address: fileviez@physics.wisc.edu

[†]Electronic address: sspinner@wisc.edu

[‡]Electronic address: trenkel@hep.wisc.edu

Contents

I. INTRODUCTION

The main goal of the Large Hadron Colllider (LHC) is to discover the mechanism responsible for elec-troweak symmetry breaking in the context of the standard model (SM) or in a new TeV scale theory. The minimal supersymmetric standard model (MSSM) is considered as one of the most appealing contenders for this new theory. In this context two important cosmological issues can be solved: the matter-antimatter asymmetry can be understood through the electroweak baryogenesis mechanism and the cold dark matter of the universe candidate may be the lightest supersymmetric particle (LSP). See Ref. [1] for a review on phenomenological and cosmological aspects of supersymmetry.

The fate of R-parity in the context of the MSSM is a central issue which has profound implications for particle physics and cosmology. R-parity is defined as $R = (-1)^{2S} M$, where S and $M = (-1)^{3(B-L)}$ are the spin and matter parity, respectively. Here B and L stand for Baryon and Lepton number. The possible implications of the conservation or violation of this discrete symmetry have been studied quite intensively in the last 30 years by many experts. See for example Refs. [2–6]. However, there are only a few phenomenological studies of theories which dynamically explain the origin of R-parity. Recently, we initiated such a study in Ref. [7] and extend its scope in this article.

The simplest way to understand the state of R-parity is in the context of a B-L extension of the MSSM, where matter parity is just a subgroup of the new abelian symmetry, $U(1)_{B-L}$. These theories are quite simple because only three copies of right-handed neutrinos are needed for an anomaly free theory. Recently, it was noticed that the minimal B-L model violates R-parity [8], a scenario further motivated by string theory [9]. However, since only experiments will reveal the validity of this symmetry, it is important to understand the second possibility as well, *i.e.* the dynamical conservation of R-parity. This is especially crucial because observation of missing energy signals at the LHC do not necessarily bare cosmological sig-nificance. Therefore, observing both missing energy and the signals discussed in this paper could increase the connection of dark matter to missing energy.

In the simplest framework for dynamical R-parity conservation, B-L is broken at the TeV scale making the model testable at the LHC. We discuss the prospects for testing the mechanism for the stability of the LSP in two different models which fit in this framework. Our key findings center around the properties of the B-L Higgs which can decay into two right-handed neutrinos in the first model and into two sfermions in the second case. The final states in the former case are especially interesting since even though R-parity is conserved, the final states can violate lepton number. Furthermore the right-handed neutrinos are long-lived giving rise to up to four displaced vertices. The main production channels for the Higgses at the LHC are investigated in detail and we discuss all possible signals one could use to test the theory of R-parity

conservation.

This work is organized as follows: In Section II we briefly summarize the main implications from R-parity conservation or violation. The simplest theoretical frameworks for R-parity conservation are discussed in Section III. In Section IV we discuss the decays of the Z_{BL} gauge boson including the effects of supersymmetric particles. All production mechanisms at the LHC for the B-L Higgses are investigated in Section V. The decays of the physical Higgses are discussed in Section VI, while in Section VII we study the most generic signals coming from R-parity conservation. Finally, we summarize our results in Section VIII.

II.   SUPERSYMMETRY, R-PARITY AND THE LHC

The signals indicating a discovery of low scale supersymmetry (SUSY) at the LHC depend on the conservation or violation of R-parity. In fact, both the cosmological and phenomenological aspects of the MSSM crucially depend on this. It is well-known that one has the following predictions:

- *R-Parity Conservation*: SUSY particles are produced in pairs and typically decay via long decay chains with multijets, multileptons and missing energy. The latter is due to the LSP, which is stable. Detecting missing energy is then a direct evidence for SUSY dark matter. However, while the LSP may be stable on collider scales, its stability on cosmological scales is not assured. If the mechanism for the LSP stability (R-parity conservation) is also tested it can shed further light on this issue [7].

- *R-Parity Breaking*: One can have single production of supersymmetric particles and possible observation of lepton and/or baryon violation at the LHC. See Ref. [5] for a review and Ref. [10–13] for recent studies. Lepton number violation stems from non-vanishing couplings of the type LH_u, LLe^c or QLd^c, while the presence of $u^c d^c d^c$ lead to baryon number violation. However, the presence of both lepton and baryon number violating terms together would lead to catastrophic proton decay [6].

  In general it is easier to discover SUSY at the LHC if R-parity is broken since SUSY particles decay to SM final states instead of missing energy, except for the SM neutrinos. In models with spontaneous R-parity breaking through the vacuum expectation value of the right-handed sneutrinos [3, 8, 14, 15], only the bilinear term LH_u from above exists at the renormalizable level. Furthermore, it is important to note that even when R-parity is broken, the gravitino can still be a good dark matter candidate [16]. We postpone discussing the LHC testability of the theories with spontaneously broken R-parity to a later article.

If SUSY is discovered at the LHC with missing energy, a possible next step is to test the mechanism responsible for R-parity conservation. In the simplest case of a gauged B-L symmetry, which we will pursue here, the following items should be searched for:

- The new neutral gauge boson, Z_{BL}, associated with the local B-L symmetry. For a review on $Z^{'}$ gauge bosons see Ref. [17]. See also Ref. [18].

- The right handed neutrinos necessary for an anomaly free gauged B-L theory and study their decays. One possibility is through the production mechanism, $pp \to Z_{BL}^{*} \to NN$. See for example Ref. [19–21] for a detailed study.

- Identify the properties of the Higgses responsible for breaking B-L. As will be discussed later, these have different relationships to the different LSPs (potential dark matter candidates) and so studying their properties may also help to identify the dark matter candidate.

There are several studies on the discovery of the first two points: $Z^{'}$ gauge bosons and right-handed neutrinos at the LHC. However, the properties of the SUSY Higgs bosons responsible for the conservation of R-parity have not been studied, except in Ref. [7], which expand upon here by studying the Higgs production and decay in more detail.

III.   THEORETICAL FRAMEWORK FOR R-PARITY CONSERVATION

The simple B-L extension of the MSSM has two different incarnations which carry a mechanism for dynamically conserving R-parity. Before addressing these, we briefly review the status of R-parity in the MSSM.

As it is well-known, the superpotential of the MSSM is given by

$$\mathcal{W}_{MSSM} = \mathcal{W}_{RpC} + \mathcal{W}_{RpV}, \tag{1}$$

where $\mathcal{W}_{RpC}$ is the R-parity conserving part

$$\mathcal{W}_{RpC} = Y_u \, \hat{Q} \, \hat{H}_u \, \hat{u}^c + Y_d \, \hat{Q} \, \hat{H}_d \, \hat{d}^c + Y_e \, \hat{L} \, \hat{H}_d \, \hat{e}^c + \mu \, \hat{H}_u \, \hat{H}_d, \tag{2}$$

and

$$\mathcal{W}_{RpV} = \epsilon \hat{L} \, \hat{H}_u + \lambda \hat{L} \, \hat{L} \, \hat{e}^c + \lambda' \hat{Q} \, \hat{L} \, \hat{d}^c + \lambda'' \hat{u}^c \, \hat{d}^c \, \hat{d}^c, \tag{3}$$

contains the R-parity violating terms. Gauging B-L forbids the terms in Eq. (3), which all violate B-L by one unit. The most straightforward possibility for the new gauge group is

$$SU(3)_C \bigotimes SU(2)_L \bigotimes U(1)_Y \bigotimes U(1)_{B-L} \tag{4}$$

Since three copies of right-handed neutrinos are needed to cancel linear and cubic B-L anomalies, the most general superpotential becomes

$$\mathcal{W}_{B-L} = \mathcal{W}_{RpC} + Y_\nu \hat{L} \hat{H}_u \hat{\nu}^c + \mathcal{W}_{extra}, \tag{5}$$

where the last term is model dependent. The particle content and its charge under Eq. (4) is that of the MSSM:

$$\hat{Q}^T = \left(\hat{u}, \hat{d} \right) \sim (3, 2, 1/6, 1/3), \qquad \hat{u}^c \sim (\bar{3}, 1, -2/3, -1/3), \qquad \hat{d}^c \sim (\bar{3}, 1, 1/3, -1/3),$$

$$\hat{L}^T = (\hat{\nu}, \hat{e}) \sim (1, 2, -1/2, -1), \qquad \hat{e}^c \sim (1, 1, 1, 1), \tag{6}$$

$$\hat{H}_u^T = \left(\hat{H}_u^+, \hat{H}_u^0 \right) \sim (1, 2, 1/2, 0), \qquad \hat{H}_d^T = \left(\hat{H}_d^0, \hat{H}_d^- \right) \sim (1, 2, -1/2, 0),$$

plus the right-handed neutrinos:

$$\hat{\nu}^c \sim (1, 1, 0, 1). \tag{7}$$

The only remaining sector left to specify is the Higgs content which serves to break $U(1)_{B-L}$ and also governs the dynamical conservation of R-parity. Here we will introduce two possibilities within the simple framework of adding only a vector-like pair of Higgses. In general, we will refer to these Higgses as

$$\hat{\bar{\phi}} \sim (1, 1, 0, \eta_\phi) \qquad \hat{\phi} \sim (1, 1, 0, -\eta_\phi). \tag{8}$$

- **Model I** ($\eta_\phi = 2$): Here we dub the Higgses $\hat{X}, \hat{\bar{X}} \sim (1, 1, 0, \pm 2)$. The extra term in the above superpotential reads as:

$$\mathcal{W}_{extra}^{(I)} = \mu_X \hat{X} \hat{\bar{X}} + f \hat{\nu}^c \hat{\nu}^c \hat{X}. \tag{9}$$

Once the Higgses acquire a VEV, the second term above induces a Majorana mass term for the right-handed neutrinos making the neutrinos Majorana fermions. Furthermore, the new Higgses can decay at tree level into two right-handed neutrinos. Recently, it was noted that radiative symmetry

breaking via the f Yukawa coupling dictates that in the majority of the parameter space R-parity is spontaneously broken [22]. In this paper, we do not subscribe to any high-scale scenario and simply assume that the Higgses acquire an R-parity conserving VEV and then study their signals at the LHC. Interestingly enough, even though R-parity is conserved, lepton number is still broken and could manifest itself in the form of same-sign leptonic final states. For lepton flavor violating rare leptonic decays, see [23]. For the study of other aspects of this model see Ref. [4, 19].

- **Model II** ($\eta_\phi = \frac{2p}{2q+1}$): While it is well-known that Higgs bosons with even B-L charge which acquire a VEV conserve R-parity [4], we supplement this by noting that $2p/(2q + 1)$ with p and q integers also conserves R-parity. This includes $\eta_\phi = 4$, $2/3$ and $4/3$ for example. This model has not been studied before and has distinctly different Higgs physics from Model I. We term the Higgses in this case $\hat{S}, \hat{\bar{S}} \sim (1, 1, 0, \pm\eta_S)$ and the extra term in the superpotential is simply the mass term:

$$\mathcal{W}_{extra}^{(II)} = \mu_S \hat{S} \hat{\bar{S}}. \tag{10}$$

Neutrinos in this case are Dirac fermions and the new physical Higgses do not couple to the MSSM superfields at tree level. This scenario is quite interesting because it is so distinct from the previous case indicating different signatures for the mechanism responsible for the stability of the LSP and give rise to very exotic Higgs signals at the LHC.

In general models of $B - L$, such as the Models I and II, kinetic mixing is possible between the Z and Z_{BL}. However the mixing is constrained to be less than about 10^{-2} and only plays a role in precision physics [24]. We therefore ignore it for the remainder of this work.

For the remainder of this section we discuss the details of these two scenarios in a general way.

A. B-L Symmetry Breaking

In order to discuss the symmetry breaking in these models in a general way, we use the notation $\phi, \bar{\phi} \sim (1, 1, 0, \pm n_\phi)$. Then, $\phi(\bar{\phi})$ can be $X(\bar{X})$ in model I or $S(\bar{S})$ in model II. The relevant soft terms for our discussions are:

$$\begin{aligned} -\mathcal{L}_{Soft} \supset & \left(a_\nu \tilde{L} H_u \tilde{\nu}^c - b_\phi \phi\bar{\phi} + \frac{1}{2} M_{BL} \tilde{B}' \tilde{B}' + \text{h.c.} \right) \\ & + m_\phi^2 |\phi|^2 + m_{\bar{\phi}}^2 |\bar{\phi}|^2 + m_{\tilde{\nu}^c}^2 |\tilde{\nu}^c|^2 + ..., \end{aligned} \tag{11}$$

where $\tilde{B}'$ is the B-L gaugino and ... indicates MSSM soft terms. Spontaneous B-L breaking and R-parity conservation require the nonzero VEVs for ϕ and $\bar{\phi}$. Notice that in the above equation one should add the trilinear term $a_f \tilde{\nu}^c \tilde{\nu}^c \phi$ in the case of Model I. Using $\langle \phi \rangle = v/\sqrt{2}$ and $\langle \bar{\phi} \rangle = \bar{v}/\sqrt{2}$ one finds

$$V = \frac{1}{2}|\mu_\phi|^2 \left(v^2 + \bar{v}^2 \right) - b_\phi v \bar{v} + \frac{1}{2}m_\phi^2 v^2 + \frac{1}{2}m_{\bar{\phi}}^2 \bar{v}^2 + \frac{g_{BL}^2}{32} n_\phi^2 \left(v^2 - \bar{v}^2 \right)^2. \tag{12}$$

This form is very similar to that of the MSSM and the derivations that follow mirror those of the MSSM with the appropriate replacements. Assuming that the potential is bounded from bellow along the D-flat direction leads to the condition:

$$2b_\phi < 2|\mu_\phi|^2 + m_\phi^2 + m_{\bar{\phi}}^2, \tag{13}$$

while

$$b_\phi^2 > \left(|\mu_\phi|^2 + m_\phi^2 \right) \left(|\mu_\phi|^2 + m_{\bar{\phi}}^2 \right). \tag{14}$$

is necessary for a nontrivial minimum. Minimizing with respect v and $\bar{v}$ one gets

$$\begin{aligned}
|\mu_\phi|^2 + m_\phi^2 - \frac{1}{2}m_{Z_{BL}}^2 \cos 2\beta' - b_\phi \cot \beta' = 0, \\
|\mu_\phi|^2 + m_{\bar{\phi}}^2 + \frac{1}{2}m_{Z_{BL}}^2 \cos 2\beta' - b_\phi \tan \beta' = 0,
\end{aligned} \tag{15}$$

with $\tan \beta' = v/\bar{v}$ and $m_{Z_{BL}}^2 = g_{BL}^2 n_\phi^2 (v^2 + \bar{v}^2)/4$. These can be recast into the more useful form:

$$\frac{1}{2}m_{Z_{BL}}^2 = -|\mu_\phi|^2 - \left(\frac{m_\phi^2 \tan^2 \beta' - m_{\bar{\phi}}^2}{\tan^2 \beta' - 1} \right), \tag{16}$$

$$b_\phi = \frac{\sin 2\beta'}{2} \left(2|\mu_\phi|^2 + m_\phi^2 + m_{\bar{\phi}}^2 \right). \tag{17}$$

From here we move on to describe the spectrum details.

B. Mass Spectrum

Higgs Bosons:

The physical Higgs content includes the MSSM Higgses: h, H, A, $H^\pm$, as well as two extra CP-even neutral Higgses, H_1 and H_2, and one CP-odd Higgs, A_ϕ (X_1, X_2 and A_{BL} in Model I and S_1, S_2 and A_S

in Model II). The complex gauge states can be written down in terms of their real components:

$$\phi = \frac{1}{\sqrt{2}}(v + \phi_R) + \frac{i}{\sqrt{2}}\phi_I, \qquad \bar{\phi} = \frac{1}{\sqrt{2}}(\bar{v} + \bar{\phi}_R) + \frac{i}{\sqrt{2}}\bar{\phi}_I, \tag{18}$$

and related to the physical states through

$$\begin{pmatrix} \phi_R \\ \bar{\phi}_R \end{pmatrix} = \begin{pmatrix} \cos\alpha' & \sin\alpha' \\ -\sin\alpha' & \cos\alpha' \end{pmatrix} \begin{pmatrix} H_1 \\ H_2 \end{pmatrix}, \tag{19}$$

$$\begin{pmatrix} \phi_I \\ \bar{\phi}_I \end{pmatrix} = \begin{pmatrix} \sin\beta' & \cos\beta' \\ -\cos\beta' & \sin\beta' \end{pmatrix} \begin{pmatrix} G_\phi \\ A_\phi \end{pmatrix}, \tag{20}$$

where G_ϕ is the Goldstone boson associated with breaking B-L and which is eaten by Z_{BL}. The Higgs spectrum is completely parameterized by: $\tan\beta', m_{Z_{BL}}$ and

$$m_{A_\phi}^2 = \frac{2b_\phi}{\sin 2\beta'}. \tag{21}$$

The eigenvalues and the mixing angles in the CP-even neutral Higgs sector read as

$$m_{H_{1,2}}^2 = \frac{1}{2}\left(m_{A_\phi}^2 + m_{Z_{BL}}^2 \mp \sqrt{(m_{A_\phi}^2 - m_{Z_{BL}}^2)^2 + 4m_{Z_{BL}}^2 m_{A_\phi}^2 \sin^2(2\beta')} \right), \tag{22}$$

$$\frac{\tan 2\alpha'}{\tan 2\beta'} = \frac{m_{A_\phi}^2 + m_{Z_{BL}}^2}{m_{A_\phi}^2 - m_{Z_{BL}}^2}. \tag{23}$$

Notice that in the limit, $m_{Z_{BL}}^2 \gg m_{A_\phi}^2$, which will be employed later, the above simplifies to

$$m_{H_1}^2 \sim m_{A_\phi}^2 \left(1 - \sin^2 2\beta' \right), \tag{24}$$

$$m_{H_2}^2 \sim m_{Z_{BL}}^2 + m_{A_\phi}^2 \sin^2 2\beta', \tag{25}$$

$$\alpha' \sim -\beta' - \frac{\tan 2\beta'}{1 + \tan^2 2\beta'} \frac{m_{A_\phi}^2}{m_{Z_{BL}}^2}. \tag{26}$$

Then, assuming a TeV scale $m_{Z_{BL}}$ and small m_{A_ϕ} one expects two light Higgses at around the same mass: H_1 and A_ϕ, and a heavy one, H_2 close to the Z_{BL} mass. Regardless of the parameter space though, the following relationships are observed: $m_{H_1} \leq m_{A_\phi}$ and $m_{Z_{BL}}$ and $m_{H_2} \geq m_{A_\phi}$ and $m_{Z_{BL}}$.

Neutrino Sector:

The neutrino sector of the two models differs dramatically so we can not discuss the two models generically in a worthwhile way. Model II is simple, in this case, neutrinos are Dirac fermions. However, in Model I, once the X and $\bar{X}$ get a VEV a Majorana mass term will be induced for the right-handed neutrinos:

$$m_{N_i} = \sqrt{2}\, f_i \sin\beta'\, \frac{m_{Z_{BL}}}{g_{BL}}, \tag{27}$$

noting that f can be diagonalized without loss of generality. This mass in turn triggers the type I seesaw mechanism for neutrino masses [25]:

$$m_\nu = \sqrt{2}\, v_u^2 Y_\nu^T (m_N)^{-1} Y_\nu. \tag{28}$$

As is typical for TeV scale seesaws, $Y_\nu \sim 10^{-6}$ correctly reproduces the neutrino masses.

Neutralino Sector:

The neutralino mass matrix, in the basis $\tilde{\psi}^0 = \left(\psi_{\mathrm{MSSM}},\ \tilde{B}',\ \tilde{\phi},\ \tilde{\bar{\phi}}\right)$, reads as:

$$\mathcal{M}_{\chi^0} = \begin{pmatrix} \mathcal{M}_{\mathrm{MSSM}} & 0 & 0 & 0 \\ 0 & M_{BL} & -g_{BL}\,\frac{n_\phi}{2}\,v & g_{BL}\,\frac{n_\phi}{2}\,\bar{v} \\ 0 & -g_{BL}\,\frac{n_\phi}{2}\,v & 0 & -\mu_\phi \\ 0 & g_{BL}\,\frac{n_\phi}{2}\,\bar{v} & -\mu_\phi & 0 \end{pmatrix}, \tag{29}$$

where ψ_{SM} defines the MSSM neutralinos and $\mathcal{M}_{\mathrm{MSSM}}$ the four-by-four MSSM neutralino mass matrix. Here, we define the mass eigenstates as in the MSSM

$$\tilde{\chi}_i^0 = N_{ij}\tilde{\psi}_j^0, \tag{30}$$

where N diagonalizes the full seven-by-seven neutralino mass matrix and breaks up into block diagonal form where the upper four-by-four block diagonalizes the MSSM and the lower three-by-three block diagonalizes the B-L neutralino sector. The eigenstates are labeled with increasing mass so that χ_1^0 (χ_7^0) is the lightest (heaviest) neutralino, although the lightest B-L neutralino will play a role later so we denote it $\tilde{\chi}_{BL}$.

Sfermion Masses:

In the sfermion sector, the mass matrices $\mathcal{M}_{\tilde{u}}^2$, $\mathcal{M}_{\tilde{d}}^2$, and $\mathcal{M}_{\tilde{e}}^2$ in the basis $\left(\tilde{f}_L,\ \tilde{f}_R\right)$ are given by

$$\begin{pmatrix} m_{\tilde{Q}}^2 + m_u^2 + \left(\frac{1}{2} - \frac{2}{3}s_W^2\right) M_Z^2\, c_{2\beta} + \frac{1}{3}D_{BL} & \frac{1}{\sqrt{2}}\left(a_u\, v_u - Y_u\, \mu\, v_d\right) \\ \frac{1}{\sqrt{2}}\left(a_u\, v_u - Y_u\, \mu\, v_d\right) & m_{\tilde{u}^c}^2 + m_u^2 + \frac{2}{3}M_Z^2\, c_{2\beta}\, s_W^2 - \frac{1}{3}D_{BL} \end{pmatrix},$$

$$
\begin{pmatrix}
m_{\tilde{Q}}^2 + m_d^2 - \left(\frac{1}{2} - \frac{1}{3} s_W^2\right) M_Z^2 c_{2\beta} + \frac{1}{3} D_{BL} & \frac{1}{\sqrt{2}} \left(Y_d\, \mu\, v_u - a_d\, v_d\right) \\
\frac{1}{\sqrt{2}} \left(Y_d\, \mu\, v_u - a_d\, v_d\right) & m_{\tilde{d}^c}^2 + m_d^2 - \frac{1}{3} M_Z^2 c_{2\beta} s_W^2 - \frac{1}{3} D_{BL}
\end{pmatrix},
\tag{31}
$$

$$
\begin{pmatrix}
m_{\tilde{L}}^2 + m_e^2 - \left(\frac{1}{2} - s_W^2\right) M_Z^2 c_{2\beta} - D_{BL} & \frac{1}{\sqrt{2}} \left(Y_e\, \mu\, v_u - a_e\, v_d\right) \\
\frac{1}{\sqrt{2}} \left(Y_e\, \mu\, v_u - a_e\, v_d\right) & m_{\tilde{e}^c}^2 + m_e^2 - M_Z^2 c_{2\beta} s_W^2 + D_{BL}
\end{pmatrix},
$$

where $c_{2\beta} = \cos 2\beta$, $s_W = \sin\theta_W$ and

$$
D_{BL} \equiv \frac{1}{8}\, g_{BL}^2 n_\phi \left(\bar{v}^2 - v^2\right) = \frac{1}{2n_\phi} M_{Z_{BL}}^2 \cos 2\beta'.
\tag{32}
$$

m_u, m_d and m_e are the respective fermion masses and a_u, a_d and a_e are the trilinear a-terms corresponding to the Yukawa couplings Y_u, Y_d and Y_e. Typically, it is assumed that substantial left-right mixing occurs only in the third generation. Regardless, the physical states are related to the gauge states by

$$
\begin{pmatrix} \tilde{q}_1 \\ \tilde{q}_2 \end{pmatrix} = \begin{pmatrix} \cos\theta_{\tilde{q}} & \sin\theta_{\tilde{q}} \\ -\sin\theta_{\tilde{q}} & \cos\theta_{\tilde{q}} \end{pmatrix} \begin{pmatrix} \tilde{q} \\ \tilde{q}^{c*} \end{pmatrix},
\tag{33}
$$

where here we are thinking about the squark sector, but, of course, the same thing can be done in the slepton sector.

The left-right mixing in the sneutrino sector is negligible due to the small Dirac Yukawa couplings necessary for the type I seesaw mechanism. The left-handed masses are

$$
m_{\tilde{\nu}_L}^2 = m_{\tilde{L}}^2 + \frac{1}{2} M_Z^2 \cos 2\beta - D_{BL}.
\tag{34}
$$

In Model I the right-handed sneutrino CP-even and CP-odd states are split by trilinear terms involving the B-L Higgses. Remembering that the Yukawa matrix, f, can be chosen to be diagonal without loss of generality, the masses of the right-handed sneutrinos are given by

$$
m_{\tilde{N}_{R_i}}^2 = m_{\tilde{\nu}_i^c}^2 + 2 f_i^2\, v^2 + \sqrt{2}\, a_{f_i}\, v + \sqrt{2}\, f_i\, \mu_X\, \bar{v} + D_{BL},
\tag{35}
$$

$$
m_{\tilde{N}_{I_i}}^2 = m_{\tilde{\nu}_i^c}^2 + 2 f_i^2\, v^2 - \sqrt{2}\, a_{f_i}\, v - \sqrt{2}\, f_i\, \mu_X\, \bar{v} + D_{BL}.
\tag{36}
$$

where i runs over all three generations and repeated indices are not summed. The masses for Model II can be recovered from the above by setting f_i, $a_{f_i} \to 0$ and in this case the right-handed sneutrino can be treated as a single complex scalar field.

It is important to reemphasize that in this context R-parity conservation and therefore the stability of

the LSP is a direct consequence of the breaking of B-L via ϕ and $\bar{\phi}$. The properties of these fields are the crucial ingredient for testing this mechanism. These can give rise to unique signals: lepton number violating in Model I (despite the conservation of R-parity) and multi-leptons and/or multi-photons in Model II.

IV.   DECAYS OF THE Z_{BL} NEUTRAL GAUGE BOSON

The discovery of a new B-L gauge boson at the LHC is crucial to establish the existence of a new abelian gauge symmetry and to test the mechanism responsible for R-parity conservation or violation in the supersymmetric case. In this section we discuss the main features of the Z_{BL} boson decays in order to understand the impact of the supersymmetric particles on the total width. Furthermore, Z_{BL} can decay into the Higgses A_{BL} and X_1, a decay that does not exist in the minimal non-SUSY B-L model (since there is no A_{BL}). As we will discuss later, this decay width also enters into the Higgs pair production cross section, $pp \to Z_{BL}^* \to H_1 A_\phi$, which is an important channel for the discovery of these fields.

The current bounds on Z_{BL} from LEP II are commonly quoted as $m_{Z_{BL}}/g_{BL} > 6$ TeV [26] but since our covariant derivative is defined as $D^\mu = \partial^\mu - \frac{1}{2} g_{BL} n_\phi Z_{BL}^\mu$, the relevant bound here is

$$\frac{m_{Z_{BL}}}{g_{BL}} > 3 \text{ TeV}. \tag{37}$$

In what follows, we will simply take this upper limit as an equality.

The Z_{BL} boson can decay into a pair of fermions, light or heavy neutrinos, sfermions, or into a pair of two new Higgs boson. The partial widths for the decay into particles P_1, P_2 of masses m_1, m_2 are given by,

$$\Gamma(Z_{BL} \to P_1 P_2) = \frac{1}{16\pi m_{Z_{BL}}} \left|\overline{\mathcal{M}}(Z_{BL} \to P_1 P_2)\right|^2 \sqrt{\left(1 - \frac{(m_1 + m_2)^2}{m_{Z_{BL}}^2}\right)\left(1 - \frac{(m_1 - m_2)^2}{m_{Z_{BL}}^2}\right)},$$
$$\tag{38}$$

where the squared matrix elements follow from the Feynman rules in the Appendix:

$$\left|\overline{\mathcal{M}}(Z_{BL} \to f_i \bar{f_i})\right|^2 = \frac{4}{3} c_f \left(\frac{g_{BL}}{2} n_{BL}^f\right)^2 m_{Z_{BL}}^2 \left(1 + \frac{2m_{f_i}^2}{m_{Z_{BL}}^2}\right), \qquad f_i = u,d,c,s,b,t,e,\mu,\tau; \tag{39}$$

$$\left|\overline{\mathcal{M}}(Z_{BL} \to \nu_i \bar{\nu_i})\right|^2 = \frac{2}{3} \left(\frac{g_{BL}}{2} n_{BL}^\nu\right)^2 m_{Z_{BL}}^2, \tag{40}$$

$$\left|\overline{\mathcal{M}}(Z_{BL} \to \bar{N} N)\right|^2 = \frac{2}{3} \left(\frac{g_{BL}}{2} n_{BL}^{\nu_R}\right)^2 m_{Z_{BL}}^2 \left(1 - 4\frac{m_N^2}{m_{Z_{BL}}^2}\right), \tag{41}$$

$$\left|\overline{\mathcal{M}}(Z_{BL} \to \tilde{f}_\alpha \tilde{f}_\beta^*)\right|^2 = \frac{1}{3} c_{\tilde{f}} \left(\frac{g_{BL}}{2} n_{BL}^{\tilde{f}}\right)^2 m_{Z_{BL}}^2 \left(1 - \frac{2m_{\tilde{f}_\alpha}^2 + 2m_{\tilde{f}_\beta}^2}{m_{Z_{BL}}^2} + \frac{\left(m_{\tilde{f}_\alpha}^2 - m_{\tilde{f}_\beta}^2\right)^2}{m_{Z_{BL}}^4}\right) \tag{42}$$

$$\times \left(U_{\alpha1}^{\tilde{f}} U_{\beta1}^{\tilde{f}} + U_{\alpha2}^{\tilde{f}} U_{\beta2}^{\tilde{f}}\right)^2, \qquad \tilde{f}_\alpha \tilde{f}_\beta^* = \tilde{q}_{i\alpha} \tilde{q}_{i\beta}^*, \tilde{l}_{i\alpha} \tilde{l}_{i\beta}^*, \tilde{\nu}_i \tilde{\nu}_i^*, \tilde{\nu}_{Ri} \tilde{\nu}_{Ri}^*;$$

$$\left|\overline{\mathcal{M}}(Z_{BL} \to X_i A_{BL})\right|^2 = \frac{1}{3} \left(\frac{g_{BL}}{2} n_{BL}^X\right)^2 m_{Z_{BL}}^2 \left(1 - \frac{2m_{X_i}^2 + 2m_{A_{BL}}^2}{m_{Z_{BL}}^2} + \frac{\left(m_{X_i}^2 - m_{A_{BL}}^2\right)^2}{m_{Z_{BL}}^4}\right) \tag{43}$$

$$\times \cos^2(\beta' - \alpha'),$$

$$\left|\overline{\mathcal{M}}(Z_{BL} \to \bar{\chi}_i \chi_j)\right|^2 = \frac{1}{3} \left(\frac{g_{BL}}{2} n_{BL}^X\right)^2 m_{Z_{BL}}^2 \left(1 - \frac{m_i^2 + m_j^2 + 6m_i m_j}{2m_{Z_{BL}}^2} - \frac{\left(m_i^2 - m_j^2\right)^2}{2m_{Z_{BL}}^4}\right) \tag{44}$$

$$\times \left(N_{i\tilde{X}} N_{\tilde{X}j}^\dagger - N_{i\tilde{X}} N_{\tilde{X}j}^\dagger\right)^2 (1 + \delta_{ij}).$$

Here, i is a generation index, c_f are color factors ($c_{q_i} = 3$, $c_{l_i} = 1$) and $U^{\tilde{f}}$ are the unitary sfermion mixing matrices introduced in Eq. (33) and N_{ij} are the neutralino mixing matrices defined in Eq. (30). Using the above expressions we show the branching ratios of Z_{BL} in Fig. 1. In order to simplify our analysis, we choose the masses of the three right-handed neutrinos, $m_{N_i} = 95\,\text{GeV}$. We consider one light squark, $m_{\tilde{t}_1} = 150\,\text{GeV}$, and one light slepton, $m_{\tilde{\tau}_1} = 150\,\text{GeV}$. All other eleven squarks, five charged and six neutral sleptons are heavy (including the three right-handed sneutrino), $m_{\tilde{q}} = m_{\tilde{l}} = 1\,\text{TeV}$. All mixing angles in the sfermion sector are set to zero for simplicity. The masses of the new neutralinos are determined by μ_X and M_{BL}, both are taken here to be 150 GeV. Only the lightest state contributes, while the heavier ones have masses very close to $m_{Z_{BL}}$ and give negligible or zero contributions. Notice that the numerical results are shown for the model I, where the Higgses breaking B-L have $n_\phi = \pm 2$.

Fig. 1 shows that once the Z_{BL} mass is above 2 TeV, the "susy threshold", the decays into superpartners can become important. In the scenario considered in Fig. 1, for $m_{Z_{BL}} = 3000$ GeV we have the following approximate leading branching ratios:

- $\sum l^+ l^- \sim 24.4\%$

- $\sum jj \sim 13.6\%$

- $\sum \nu\nu$, $\sum NN \sim 12.2\%$
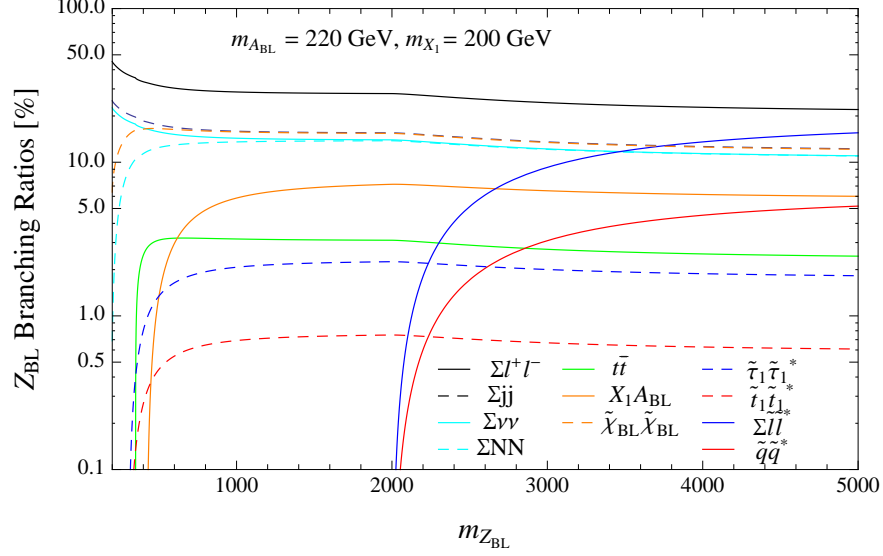
- SUSY $\sim 28.5\%$

FIG. 1: Branching ratios of the Z_{BL} boson for $m_{A_{BL}} = 220\,\text{GeV}$ and $m_{X_1} = 200\,\text{GeV}$. The masses of the three right-handed neutrinos are $m_{N_i} = 95\,\text{GeV}$. We consider one light squark, $m_{\tilde{t}_1} = 150\,\text{GeV}$, and one light slepton, $m_{\tilde{\tau}_1} = 150\,\text{GeV}$, all other eleven squarks, five charged and six neutral sleptons are heavy (including the three right-handed sneutrinos), $m_{\tilde{q}} = m_{\tilde{l}} = 1\,\text{TeV}$. All mixing angles in the sfermion sector are set to zero. The neutralino masses are determined by μ_X and M_{BL}, both taken here to be $150\,\text{GeV}$.
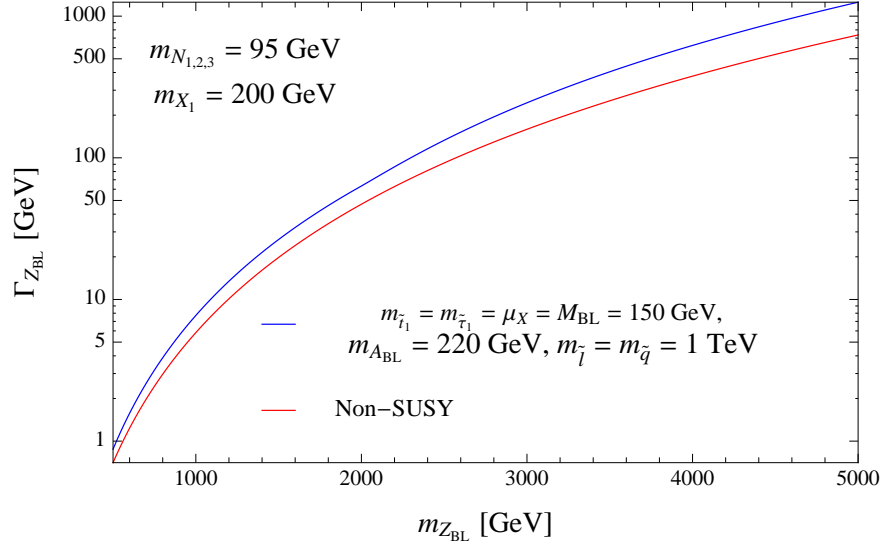

FIG. 2: The total Z_{BL} decay width as a function of the Z_{BL} mass for a a SUSY spectrum with an A_{BL} mass of 220 GeV, the lightest stop and lightest stau mass of 150 GeV and all other sfermions at 1 TeV in blue and $\mu_X = M_{BL} = 150$ GeV determine the neutralino masses. In red, for comparison, is the total width for the non-SUSY case. Note that while the decay to X_1 and A_{BL} is not a SUSY decay, it does not exist in the minimal non-SUSY B-L model. In both cases, all three right-handed neutrinos are assumed to be degenerate with a mass of 95 GeV and $m_{X_1} = 200$ GeV.

The total decay width of the Z_{BL} is shown in Fig. 2 assuming all three right-handed neutrinos are degenerate with a mass of 95 GeV and the maximum value of g_{BL} consistent with LEP II. In order to further investigate the impact of the supersymmetric particles on the total decay width, we compare the total width for a given
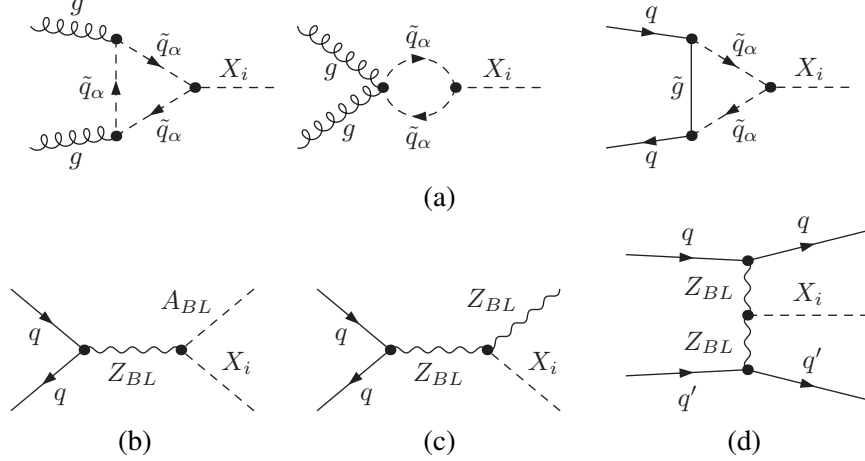
FIG. 3: Parton-level Feynman diagrams for the production of the CP-even Higgs X_i at lowest order, via (a) single production (gluon–gluon fusion or $q\bar{q}$ annihilation), (b) $A_{BL}X_i$ pair production, (c) associated $Z_{BL}X_i$ production, and (d) Z_{BL} boson fusion. For (d), the diagram with crossed external lines is not shown explicitly. The initial state particles q, q' can be any of the light-flavor quarks or antiquarks.

SUSY spectrum (blue line) with the non-SUSY case (red line). For Z_{BL} masses above the SUSY spectrum, the decays into supersymmetric particles contribute significantly and the decay widths can have significant variation between the two cases.

The key difference in the above for Model II is the different value of n_ϕ and the Dirac nature of the neutrinos. In this case, the Z_{BL} decay width to Dirac neutrinos is simply given by Eq. (39). However, the main features of the supersymmetric contribution to the branching rations and total width are similar.

V. PRODUCTION MECHANISMS OF THE B-L HIGGS BOSONS

The dominant contributions to B-L Higgs production arise from the single CP-even production via gluon fusion and pair production of the CP-even and CP-odd Higgses. Subdominant channels are associated $X_i Z_{BL}$ production and Z_{BL} boson fusion. The corresponding parton-level Feynman diagrams are shown in Fig. 3.

In the following we focus on the production of the lighter of the B-L Higgs bosons, X_1, in Model I. The production cross sections for the heavier Higgs boson, X_2, follow in complete analogy by replacing the corresponding couplings, but they are suppressed by the heavy mass and thus do not play an important role for our phenomenological studies. The results for Model II follow by scaling with the corresponding B-L factor.

A. Single Production via Gluon Fusion

Single production is possible at the one-loop level via gluon-gluon fusion, $gg \to X_1$, where squarks run inside the loop, see Fig. 3 (a) and $q\bar{q} \to X_1$, at one-loop level mediated by a gluino–squark loop, see the last graph in Fig. 3, but this contribution is highly suppressed by the light quark masses and we neglect it. Both these channels depend on SUSY interactions of gauge coupling strengths between the Higgs and squarks: the D-terms.

The cross sections for the single production can be given in analogue to Higgs boson production within the MSSM [27, 28], making sure to include only the relevant diagrams from Fig. 3. The cross section is related to the decay width of the scalar and at partonic level it is given by

$$\hat{\sigma}_{gg \to X_1} = \frac{\pi^2}{8m_{X_1}^3} \, \Gamma_{X_1 \to gg} \, \delta\left(1 - \frac{m_{X_1}^2}{\hat{s}}\right), \tag{45}$$

where $\hat{s}$ is the partonic center-of-mass energy squared. The decay width can be written as

$$\Gamma_{X_1 \to gg} = \frac{\alpha_s^2 \, m_{X_1}^3}{128\pi^3} \left| \sum_{\tilde{q}_\alpha} g_{\tilde{q}_\alpha}^{X_1} \, \frac{1}{m_{\tilde{q}_\alpha}^2} \, A(\tau_{\tilde{q}_\alpha}) \right|^2, \tag{46}$$

with $\tau_{\tilde{q}} = 4m_{\tilde{q}}^2/m_{X_1}^2$ in terms of the kinematic function $A(\tau) = -\frac{1}{2}\,\tau\,(1 - \tau f(\tau))$, and

$$f(\tau) = \begin{cases} \arcsin^2\left(\frac{1}{\sqrt{\tau}}\right), & \tau \geq 1 \\ -\frac{1}{4}\left(\log \frac{1+\sqrt{1-\tau}}{1-\sqrt{1-\tau}} - i\pi\right)^2, & \tau < 1. \end{cases} \tag{47}$$

The sum in Eq.(45) runs over all twelve squark eigenstates and the couplings $g_{\tilde{q}_\alpha}^{X_1} \equiv g_{\tilde{q}_\alpha \tilde{q}_\alpha}^{X_1}$ are given in the appendix. Note that only the diagonal $X\tilde{q}\tilde{q}$ couplings enter since the $g\tilde{q}\tilde{q}$ couplings preserve gauge and mass eigenstate of the squarks.

The couplings for the two eigenstates of a given squark $\tilde{q}_\alpha = \tilde{q}_{1,2}$ only differ by sign. This allows us to rewrite Eq.(45) as:

$$\hat{\sigma}_{gg \to X_1} = \frac{\alpha_s^2}{1024\pi} \left| \sum_{\tilde{q}} g_{\tilde{q}_1}^{X_1} \left(\frac{1}{m_{\tilde{q}_1}^2} A(\tau_{\tilde{q}_1}) - \frac{1}{m_{\tilde{q}_2}^2} A(\tau_{\tilde{q}_2})\right) \right|^2 \delta\left(1 - \frac{m_{X_1}^2}{\hat{s}}\right), \tag{48}$$

where now the sum runs over the six squark flavors. From this result one can see that in the case of degenerate squark masses, $m_{\tilde{q}_1} = m_{\tilde{q}_2}$, the contributions cancel within each squark flavor, due to the opposite B-L charges of the left- and right-handed squarks.
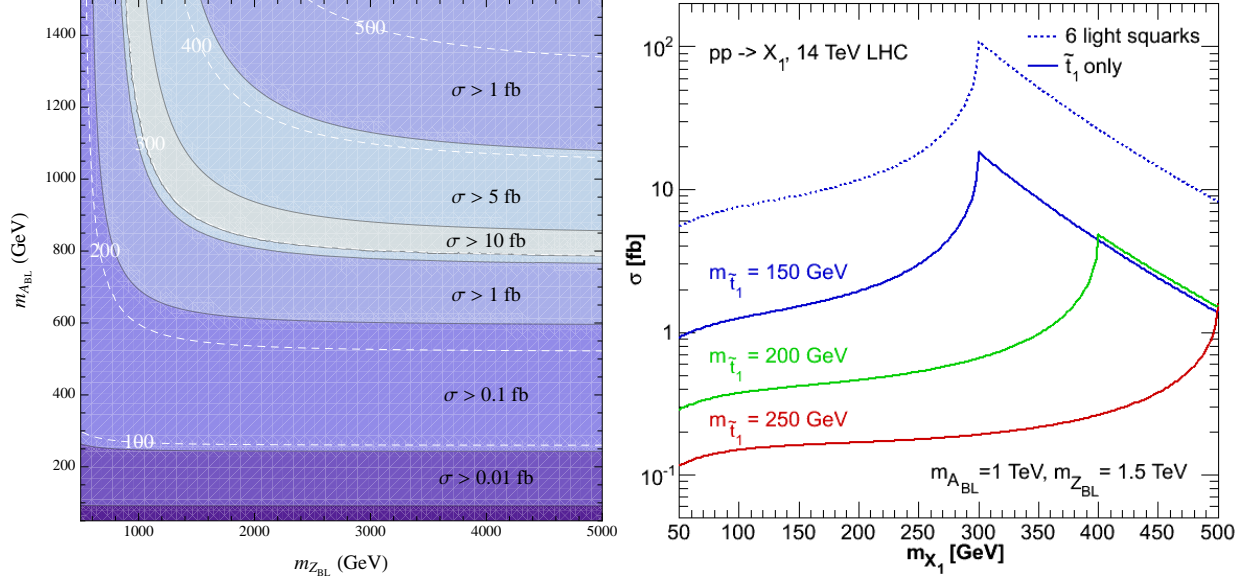
FIG. 4: Hadronic cross sections for single X_1 production at the LHC. One squark is considered to be light, $m_{\tilde{t}_1} = 150$ GeV and squark mixing is neglected. We use the MSTW 2008 LO pdf [29] at a central factorization scale $\mu = m_{X_1}/2$. In the left panel, plot lines of constant cross section in the $m_{A_{BL}} - m_{Z_{BL}}$ with fixed $\tan\beta' = 1.5$ in black and in white are lines of constant X_1 mass. In the right panel, the cross section is shown as a function of m_{X_1} for $m_{A_{BL}} = 1$ TeV and $m_{Z_{BL}} = 1.5$ TeV. Here we also explore the possibility of six light quarks (dotted) and the effects of changing the lightest stop mass (solid).

At the hadronic level, the cross section is obtained from the partonic one by the convolution,

$$\sigma_{pp \to X_1}(s) = \int_{\tau_0}^{1} d\tau \, \frac{d\mathcal{L}_{gg}^{pp}}{d\tau} \, \hat{\sigma}_{gg \to X_1} \tag{49}$$

with $\tau = \hat{s}/s$, s being the hadronic center-of-mass energy squared, and $\tau_0 = m_{X_1}^2/s$ is the production threshold. The parton luminosities are given by,

$$\frac{d\mathcal{L}_{ab}^{AB}}{d\tau} = \frac{1}{1 + \delta_{ab}} \int_{\tau}^{1} \frac{dx}{x} \left[f_{a/A}(x, \mu) \, f_{b/B}\left(\frac{\tau}{x}, \mu\right) + f_{a/B}\left(\frac{\tau}{x}, \mu\right) f_{b/A}(x, \mu) \right], \tag{50}$$

where the parton distribution functions (pdfs) $f_{a/A}(x, \mu)$ parameterize the probability of finding a parton a inside a hadron A with faction x of the hadron momentum at a factorization scale μ. In Fig. 4 numerical predictions for the single Higgs production cross section via gluon fusion are given. The cross section depends strongly on the supersymmetric spectrum.

We consider here the conservative case where only one squark is light ($m_{\tilde{t}_1} = 150$ GeV) and all other squarks are heavy and degenerate in mass and thus cancel each others contributions. In the left panel we show the curves of constant cross section in the $m_{A_{BL}} - m_{Z_{BL}}$ plane for fixed $\tan\beta' = 1.5$ in black. Lines of constant X_1 mass are shown in white. The plot reflects the sharply peaked nature of the $A(\tau)$ function

from Eq. (46) at $m_{X_1} = 2m_{\tilde{t}_1}$ where the cross section can rise to about 16 fb but then rapidly decreases when lowering the mass of X_1 due to the function $A(\tau)$ and when raiding the mass of X_1 due to both $A(\tau)$ and the decreased gluon luminosity.

In Fig. 4 (right panel) the cross section is given as a function of the Higgs mass m_{X_1}, for fixed input parameters $m_{A_{BL}} = 1$ TeV and $m_{Z_{BL}} = 1.5$ TeV and one light squark, the stop (solid lines) and shows the effects of increasing the stop mass. The cross section is very sensitive to the stop mass and decreases quickly for heavier squark masses. To the left of the peak, the suppression is due to the function $A(\tau)$ while on peak and to the right its due to the decreased gluon luminosity. For illustrative purposes we also consider the most optimistic case in which one squark of each flavor is light, *i.e.* six light squarks (dashed line). As one can read from Eq.(48), the result simply scales by six, the number of light squarks. In this case the cross section reaches 10^2 fb. Unfortunately, this production channel strongly depends on the SUSY spectrum and therefore does not allow for general predictions to test the mechanism behind R-parity conservation. An interesting property of this channel though is that a light Z_{BL} is not necessary for production. This is different for the pair production discussed in the next subsection, which does not depend very strongly on the SUSY spectrum.

B. Higgs Pair Production: $pp \rightarrow X_1 A_{BL}$

The Higgs pair production mechanism is the most important channel for our study and part of its interests stems from the fact that while it is not a SUSY process and is fairly independent of the SUSY spectrum (only via the Z_{BL} width), it does not exist in minimal non-SUSY B-L models. The reason is of course familiar to SUSY practitioners, namely that SUSY requires vector like pairs of Higgses since these scalar fields have corresponding fermionic fields which contribute to the triangle anomalies. Therefore, a minimal non-SUSY theory has only one CP-odd scalar which becomes the longitudinal component of the Z_{BL} while in SUSY there are two, one of them physical. To our knowledge and we believe for this reason, this process has not yet been discussed in the literature. The production process proceeds via

$$q(p_1)\,\bar{q}(p_2) \rightarrow X_1(p_3)\,A_{BL}(p_4). \tag{51}$$

The differential partonic cross sections is given by the spin- and color-averaged squared matrix element,

$$d\hat{\sigma}_{q\bar{q}\rightarrow X_1 A_{BL}}(\hat{s}) = \left|\overline{\mathcal{M}}_{q\bar{q}\rightarrow X_i A_{BL}}(\hat{s})\right|^2 \frac{d\mathrm{PS}^{(2)}}{2\hat{s}}, \tag{52}$$
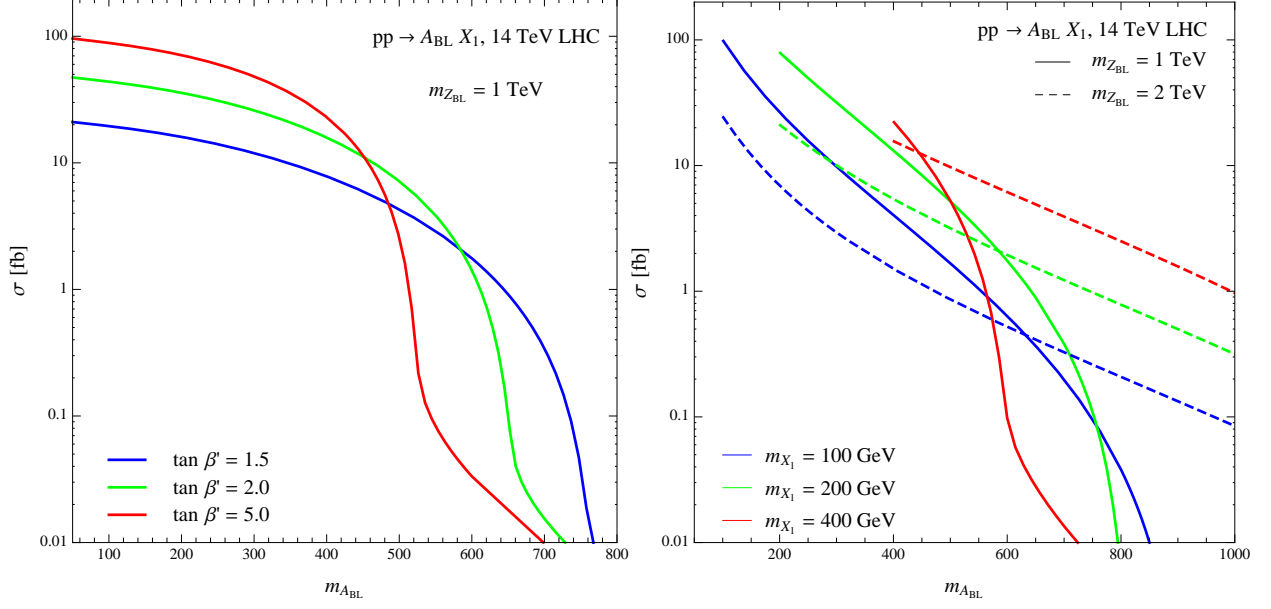
FIG. 5: A_{BL} and X_1 pair production hadronic cross section for 14 TeV center of mass energy at the LHC as a function of the mass $m_{A_{BL}}$ for fixed values of $\tan\beta'$ (left) and for fixed values of the Higgs mass m_{X_1} (right). We use the MSTW 2008 LO pdf [29] at a central factorization scale $\mu = (m_{A_{BL}} + m_{X_1})/2$. The suppression due to the threshold $m_{A_{BL}} + m_{X_1} = m_{Z_{BL}}$ is apparent in the solid lines of both plots. The key feature of this production mechanism is that it is fairly independent of the SUSY spectrum and that it can be large for a sizable part of the parameter space.

where $\mathrm{dPS}^{(2)} = d\hat{t}/(8\pi\hat{s})$ is the two-particle phase-space element. The hadronic cross section follows by convolution with the parton luminosities,

$$d\sigma_{pp \to X_1 A_{BL}}(s) = \sum_{q=u,c,d,s} \int_{\tau_0}^{1} d\tau \frac{d\mathcal{L}_{q\bar{q}}^{pp}}{d\tau} d\hat{\sigma}_{q\bar{q} \to X_i A_{BL}}(\hat{s}), \tag{53}$$

with the threshold being $\tau_0 = (m_{X_1} + m_{A_{BL}})^2/s$. It is convenient to express the matrix element in terms of the usual Mandelstam invariants,

$$\hat{s} = (p_1 + p_2)^2, \quad \hat{t} = (p_1 - p_3)^2, \quad \hat{u} = (p_1 - p_4)^2. \tag{54}$$

The squared matrix element can then be written as,

$$\left|\overline{\mathcal{M}}_{q\bar{q} \to X_1 A_{BL}}(\hat{s})\right|^2 = \frac{1}{54}\left(\frac{g_{BL}^2 n_{BL}^X}{2}\right)^2 \frac{\hat{t}\hat{u} - m_{A_{BL}}^2 m_{X_1}^2}{(\hat{s} - m_{Z_{BL}}^2)^2 + m_{Z_{BL}}^2 \Gamma_{Z_{BL}}^2} \cos^2\left(\beta' - \alpha'\right). \tag{55}$$

The numerical cross section results for the pair production of A_{BL} and X_1 at the LHC at 14 TeV are shown in Fig. 5 as a function of the mass $m_{A_{BL}}$. We use the MSTW 2008 LO pdf at a central factorization scale $\mu = (m_{A_{BL}} + m_{X_1})/2$. In both plots we use $g_{BL} = m_{Z_{BL}}/(3\text{TeV})$. In the left panel we plot the pair production cross section versus the mass of A_{BL} for three different values of $\tan\beta'$ for a fixed
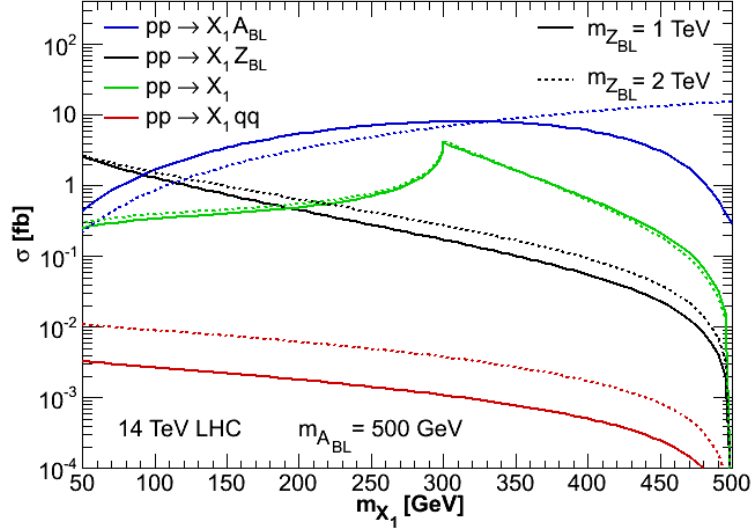
FIG. 6: Summary of all production channels for X_1 production at the LHC for $m_{A_{BL}} = 500\,\text{GeV}$ (right). One squark is assumed to be light, $m_{\tilde{t}_1} = 150$ GeV (no mixing), the heavy neutrino masses are set to $m_{\nu_R} = 95\,\text{GeV}$. We use the MSTW 2008 LO pdf at a central factorization scale (half of the final state masses).

Z_{BL} mass of 1 TeV. With these three numbers the entire Higgs sector is fixed and specifically the mass of X_1 can be calculated at each point and the larger $\tan\beta'$ the closer X_1 and A_{BL} are in mass, with $m_{A_{BL}} > m_{X_1}$. This specific parameterization has the advantage that the coupling associated with this cross section, $\cos(\beta' - \alpha')$ is relatively constant over the range of $m_{A_{BL}}$ shown and so the suppression in the cross section for increased in $m_{A_{BL}}$ is due in small part to the kinematics and in larger part to the Z_{BL} threshold ($m_{A_{BL}} + m_{X_1} = m_{Z_{BL}}$) at which point the Z_{BL} becomes off-shell and the cross section loses its resonance enhancement.

In the right panel, we show the pair production cross section versus $m_{A_{BL}}$ for three different values of m_{X_1} all for two different values of $m_{Z_{BL}}$ ($m_{Z_{BL}} = 1$ TeV solid lines and $m_{Z_{BL}} = 2$ TeV dashed). The curves start at the point $m_{A_{BL}} = m_{X_1}$ since the CP-even Higgs is at most as heavy as the CP-odd Higgs. This plot has the advantage of being in terms of the more physical parameter, m_{X_1} but then in this case, the coupling, $\cos(\beta' - \alpha')$ changes considerably over the range shown and contributes to the decrease in cross section with increasing $m_{A_{BL}}$, as does the kinematics.

In general the cross section for Higgs pair production can be sizable in a large fraction of the parameter space. For example, when the $m_{Z_{BL}} = 1$ TeV, $m_{A_{BL}}$ smaller than 500 GeV and $\tan\beta' > 1.5$ the cross section reaches several tens of femtobarn. Such results are promising for the prospects of testing the mechanism for R-parity conservation.

In order to complete our analysis we compare in Fig. 6 all of the possible production mechanisms, including the associate $Z_{BL}X_1$ production and Z_{BL} vector boson fusion. The formulas for the latter two

processes are given in Appendix A 2. In most of the considered parameter range, the $X_1 A_{BL}$ pair production dominates and the single production (for $m_{\tilde{t}_1} = 150\,\text{GeV}$) is at a similar order of magnitude. The cross section for associate $Z_{BL} X_1$ production can be large for light particle but drops off quickly for higher masses. The Z_{BL} vector boson fusion, being a $2 \rightarrow 3$ particle process, is suppressed from the kinematics and only reaches the 10^{-2} fb level. In terms of testing the mechanism for R-parity conservation the latter two channels play a subleading role and we therefore focus only on the single X_1 and $X_1 A_{BL}$ productions, which have the best potential of shedding light on the stability of the LSP. In the reminder of the paper we will discuss the subsequent decays of the B-L Higgs bosons and the signals for the B-L Higgs production at the LHC.

VI. HIGGS DECAYS AND LEPTON NUMBER VIOLATING DECAYS

The decays of the Higgses depend heavily on the spectrum. Here, we will assume that masses are such that tree-level two-body decays are open and dominate. The decays can, of course, be very different in the two models:

Model I:

The two-body decays open to X_1 are:

- $X_1 \rightarrow NN$,

- $X_1 \rightarrow \tilde{f}\tilde{f}^*$,

- $X_1 \rightarrow \tilde{\tilde{\chi}}_i \tilde{\chi}_j$.

Since the coupling of the Higgs to right-handed neutrinos is the defining characteristic of Model I, we will assume for the rest of the paper that only the first channel is open and that the SUSY decays are not kinematically allowed, namely, $m_{X_1} < 2\, m_{\text{LSP}}$. For heavier right-handed neutrinos, three general possibilities exist: decay to one right-handed neutrino and one off-shell right-handed neutrino ($m_N < m_{X_1} < 2\, m_N$), decays into two off-shell right-handed neutrinos ($m_{X_1} < m_N$) or decays similar to Model II. Off-shell right-handed neutrinos will manifest as missing energy in final states due to their mixing with the left-handed neutrinos.

The CP-odd scalar, A_{BL}, has the following potential two-body decays:

- $A_{BL} \rightarrow NN$,

- $A_{BL} \rightarrow \tilde{\tilde{\chi}}_i \tilde{\chi}_j$.

- $A_{BL} \to Z_{BL}X_1$,

where the last one would require a heavy A_{BL} outside the reach of the LHC. The two sfermion channel is missing here (compared to X_1 decays) since it stems from the D-terms in which A_{BL} does not participate. Since A_{BL} is heavier than X_1 and we have already assumed that the right-handed neutrino channel is opened to X_1 it will also be opened to A_{BL} and we proceed by assuming that all others are closed so that A_{BL} decays 100% to right-handed neutrinos.

Therefore, under our assumptions here, the relevant signals to study for Model I are the ones due to the decays of right-handed neutrinos, which we will conduct in the next subsection. As we will see, these decays could lead to lepton number violating signals due to the Majorana nature of the right-handed neutrinos.

Model II:

The difference in the second scenario is the lack of the right-handed neutrino–Higgs coupling, thereby only leaving: $S_1 \to \bar{\chi}\chi$ and $S_1 \to \tilde{f}^*\tilde{f}$ as possible tree-level two-body decays. If these are not accessible, one or more of the following decays will dominate:

- $S_1 \to \gamma\gamma$ — through a slepton and/or squark loop,

- $S_1 \to gg$ — through a squark loop,

- $S_1 \to Z_{BL}^* Z_{BL}^* \to$ some combination of leptons and jets (leptons more likely).

The CP-odd Higgs now has only two possible decays: $A_S \to \tilde{\bar{\chi}}_i \chi_j$ and $A_S \to Z_{BL}S_1$. Both decays are likely to be outside the kinematic range of the light A_S we are considering so that one of the final state particles in each of these will have to be off shell. Since the latter is independent of the SUSY spectrum, we will assume it is the dominate decay with the Z_{BL} off-shell so that the following decays are possible

- $A_S \to S_1 Z_{BL}^* \to S_1 \ell^\pm \ell^\mp$,

- $A_S \to S_1 Z_{BL}^* \to S_1 \nu\nu$.

- $A_S \to S_1 Z_{BL}^* \to S_1 jj$.

Therefore, we will assume these three body decays for A_S and two body decays for S_1, specifically the scenarios where the lightest Higgs, S_1, decays into two sleptons:

- $S_1 \to \tilde{e}\tilde{e}^*$,

- $S_1 \to \tilde{\nu}^c \tilde{\nu}^{c*}$.

The final states will depend on the identity of the LSP (potentially the dark matter candidate of the universe). We will consider the following possibilities: neutralino, gravitino and right-handed sneutrino and their associated signals.

A. Heavy Neutrinos Decays

Higgses decaying mainly into two right-handed neutrinos allow for lepton number violating signals due to the subsequent decay of the heavy Majorana right-handed neutrinos. The leading decay channels for the three heavy neutrinos, N_a, include:

$$N_a \to \ell_i^\pm W^\mp, \ \ N_a \to \nu_\ell Z, \ \ N_a \to \nu_\ell h_k, \ \ N_a \to \ell^\pm H^\mp. \tag{56}$$

The amplitude for the two first channels are proportional to the mixing between the leptons and heavy neutrinos, while the last one is proportional to the Dirac-like Yukawa terms. While decays to all the MSSM Higgses are possible, typically, only the lightest MSSM Higgs, h, is light enough for the scenario we consider here ($m_{N_a} < 500$ GeV) and so we will only take it into account. The partial decay widths of the heavy Majorana neutrinos N_i are then given by [21, 30]

$$\Gamma^{\ell W_L} \equiv \Gamma(N_a \to \ell^\pm W_L^\mp) = \frac{g^2}{64\pi M_W^2}|V_{\ell a}|^2 m_{N_a}^3 \left(1 - \frac{m_W^2}{m_{N_a}^2}\right)^2, \tag{57}$$

$$\Gamma^{\ell W_T} \equiv \Gamma(N_a \to \ell^\pm W_T^\mp) = \frac{g^2}{32\pi}|V_{\ell a}|^2 m_{N_a} \left(1 - \frac{m_W^2}{m_{N_a}^2}\right)^2, \tag{58}$$

$$\Gamma^{\nu_\ell Z_L} \equiv \Gamma(N_a \to \nu_\ell Z_L) = \frac{g^2}{64\pi M_W^2}|V_{\ell a}|^2 m_{N_a}^3 \left(1 - \frac{m_Z^2}{m_{N_a}^2}\right)^2, \tag{59}$$

$$\Gamma^{\nu_\ell Z_T} \equiv \Gamma(N_a \to \nu_\ell Z_T) = \frac{g^2}{32\pi c_W^2}|V_{\ell a}|^2 m_{N_a} \left(1 - \frac{m_Z^2}{m_{N_a}^2}\right)^2, \tag{60}$$

$$\Gamma^{\nu_\ell h} \equiv \Gamma(N_a \to \nu_\ell h) = \frac{g^2}{64\pi M_W^2}|V_{\ell a}|^2 m_{N_a}^3 \left(1 - \frac{m_h^2}{m_{N_a}^2}\right)^2. \tag{61}$$

Here the leptonic mixing between the SM charged leptons ($\ell = e, \mu, \tau$) and heavy neutrinos ($N = 1, 2, 3$) reads as [21]:

$$V_{\ell N} = V_{PMNS} \, m_\nu^{1/2} \, \Omega \, M_N^{-1/2}, \tag{62}$$

a product of matrices related to the neutrino sector. V_{PMNS} is the PMNS active neutrino mixing matrix. Under the assumption that it is real:

$$V_{PMNS} = \begin{pmatrix} c_{12}\,c_{13} & c_{13}\,s_{12} & s_{13} \\ -c_{23}\,s_{12} - c_{12}\,s_{13}\,s_{23} & c_{12}\,c_{23} - s_{12}\,s_{13}\,s_{23} & c_{13}\,s_{23} \\ s_{12}\,s_{23} - c_{12}\,c_{23}\,s_{13} & -c_{12}\,s_{23} - c_{23}\,s_{12}\,s_{13} & c_{13}\,c_{23} \end{pmatrix}, \tag{63}$$

where $c_{ij} = \cos\theta_{ij}$ and $s_{ij} = \sin\theta_{ij}$ with $0 \le \theta_{ij} \le \pi/2$. For our numerical predictions we assume the tri-bimaximal ansatz:

$$s_{12}^2 = \frac{1}{3}, \qquad s_{13}^2 = 0, \qquad s_{23}^2 = \frac{1}{2}. \tag{64}$$

The physical neutrino masses are contained in $m_\nu = diag(m_{\nu_1}, m_{\nu_2}, m_{\nu_3})$. As it is well-known, there are two possible neutrino spectra:

$$\text{Normal Hierarchy (NH):} \quad m_{\nu_1}, \;\; m_{\nu_2} = \sqrt{m_{\nu_1}^2 + \Delta m_{21}^2}, \;\; m_{\nu_3} = \sqrt{m_{\nu_1}^2 + |\Delta m_{31}^2|};$$
$$\text{Inverted Hierarchy (IH):} \quad m_{\nu_1} = \sqrt{m_{\nu_3}^2 + |\Delta m_{31}^2|}, \;\; m_{\nu_2} = \sqrt{m_{\nu_1}^2 + \Delta m_{21}^2}, \;\; m_{\nu_3}; \tag{65}$$

where [31]

$$7.27 \times 10^{-5}\text{eV}^2 \le \Delta m_{21}^2 \le 8.03 \times 10^{-5} \text{ eV}^2, \tag{66}$$

$$2.17 \times 10^{-3} \text{ eV}^2 < |\Delta m_{31}^2| < 2.54 \times 10^{-3} \text{ eV}^2, \tag{67}$$

are the solar and atmospheric mass squared differences, respectively. In this paper, we will only use the central value for these masses. Finally, Ω [32] is a complex orthogonal matrix, which conveniently parameterizes the leftover unknown degrees of freedom of the neutrino sector. We shall proceed by assuming Ω to be real. In this case it can be parameterized by three values:

$$\Omega = \begin{pmatrix} \sqrt{1-\omega_{21}^2} & -\omega_{21} & 0 \\ \omega_{21} & \sqrt{1-\omega_{21}^2} & 0 \\ 0 & 0 & 1 \end{pmatrix} \begin{pmatrix} \sqrt{1-\omega_{31}^2} & 0 & -\omega_{31} \\ 0 & 1 & 0 \\ \omega_{31} & 0 & \sqrt{1-\omega_{31}^2} \end{pmatrix} \begin{pmatrix} 1 & 0 & 0 \\ 0 & \sqrt{1-\omega_{32}^2} & -\omega_{32} \\ 0 & \omega_{32} & \sqrt{1-\omega_{32}^2} \end{pmatrix}. \tag{68}$$

Since the penultimate final states of interest are composed of right-handed neutrinos, investigating their decay properties are worthwhile, especially since they depend on the very small neutrino parameter $V_{\ell a}$. In Fig. 7 we do this by plotting the decay length in millimeters versus the mass of the right-handed neutrino (N_1

	N_1	N_2	N_3
$\mathrm{BR}(N_i \to e^- W^+)$	31.9%	15.9%	0%
$\mathrm{BR}(N_i \to \mu^- W^+)$	8.0%	15.9%	23.9%
$\mathrm{BR}(N_i \to \tau^- W^+)$	8.0%	15.9%	23.9%
$\sum \mathrm{BR}(N_i \to \nu Z)$	4.3%	4.3%	4.3%

TABLE I: Branching ratios for the right-handed neutrinos in the special case of tri-bimaximal mixing, central values for the squared mass differences and $\Omega = \mathbf{1}$ for degenerate right-handed neutrinos masses of 95 GeV.

- red, N_2 - blue and N_3 - black) in the NH (IH) on the left (right). We scan over the unknown parameters: lightest left-handed neutrino mass between 10^{-4} eV and 0.4 eV (where the latter is the upper bound from cosmology) and $0 \le \omega_{ij} \le 1$ for $i, j = 1..3$. The decay length always increases with decreasing lightest neutrino mass for all other parameters constant.

The noteworthy result from Fig. 7 is that for this range of right-handed neutrino masses— a mass range chosen to be consistent with a B-L Higgs being produced at the LHC and decay into two on-shell right-handed neutrinos —the right-handed neutrinos are long-lived (order of millimeter or above) and their decays would exhibit displaced vertices. This is a robust prediction that would lead to spectacular signals and could play a major role in distinguishing these channels. We will expand on this in the next section.

As can be appreciated from the above, the right-handed neutrino decays can be quite different in a given neutrino mass spectrum. To simplify our analysis, we will assume the following: $\Omega = \mathbf{1}$ and that the right-handed neutrinos are degenerate in mass. This is in addition to our earlier stated assumptions of tri-bimaximal mixing and central values for the squared mass differences. Ref. [21] studies the effects of varying these values on the decays of the right-handed neutrinos.

Under these assumptions the branching ratios are straightforward and independent of the mass of the lightest neutrino and the neutrino mass hierarchy and are displayed in Table I for degenerate right-handed neutrino masses of 95 GeV. These branching ratios would change as the right-handed neutrino mass increases due to the increase in strength of the Z channels and eventually the Higgs channel —kinematically not allowed for these masses— and would eventually level off. Clearly, the branching ratios mirror the tri-bimaximal mixing due to $\Omega = \mathbf{1}$.

These considerations will impact the final states and therefore the signal. We elaborate on this using the simplifying neutrino sector assumptions mentioned above and focusing on the single X_1 production and the pair production of X_1 and A_{BL}. In both cases, the Higgses decay into two right-handed neutrinos which subsequently decay into two leptons and two heavy vector bosons. The latter will further decay into jets or leptons. The signals we will focus on in the next section are the one associated with lepton number violation: the two right-handed neutrino decaying into like-sign leptons (muons or electrons) and W bosons, which
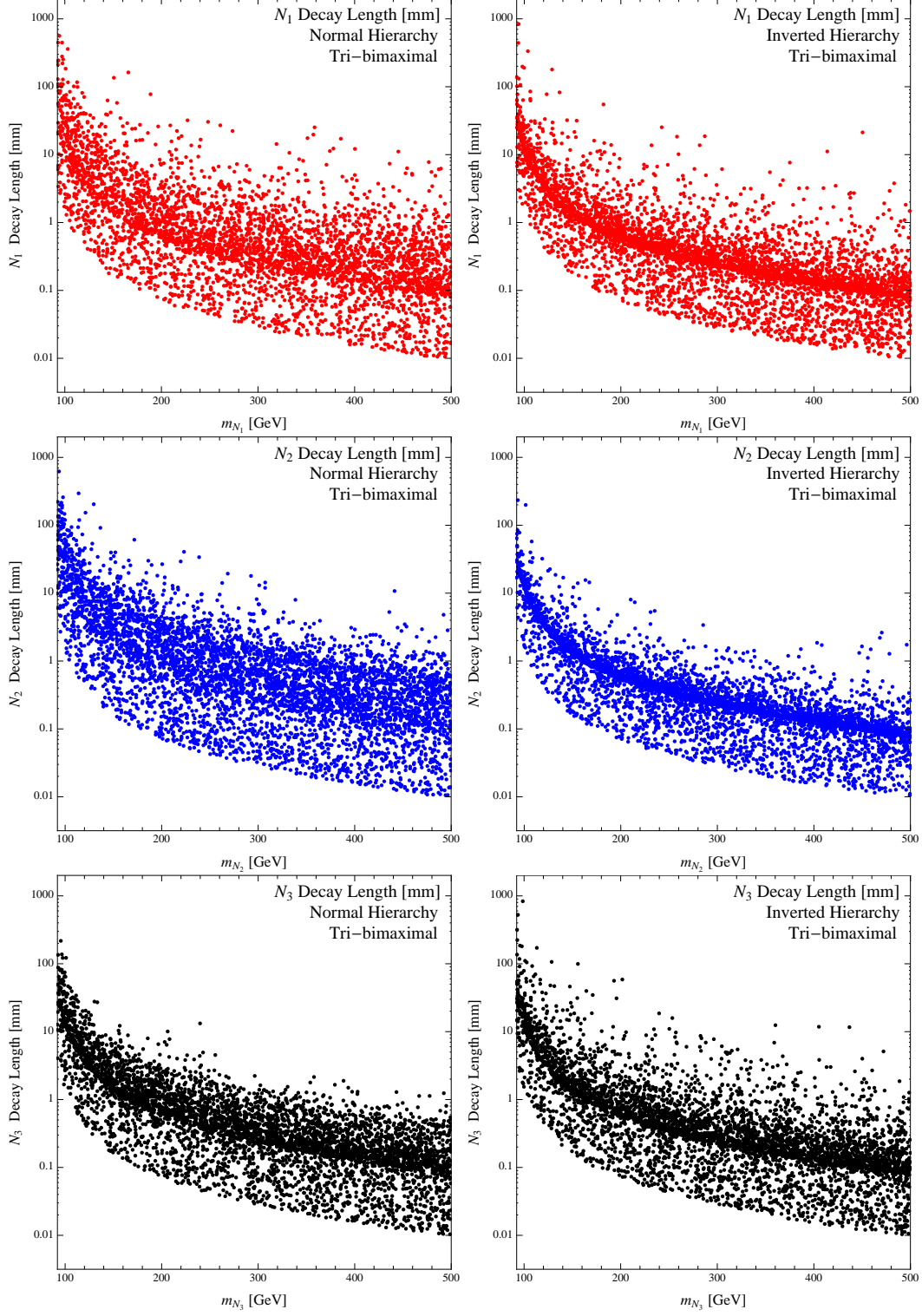
FIG. 7: The decay length for the right-handed neutrinos (N_1 - red, N_2 - blue and N_3 - black) versus their mass in the normal hierarchy (inverted hierarchy) on the left (right). We scan over the following parameters: lightest neutrino mass between 10^{-4} eV and 0.4 eV and $0 \leq \omega_{ij} \leq 1$ for $i,j = 1..3$. Due to the small right-handed left-handed neutrino mixing which facilitate these decays, the right-handed neutrinos can be quite long-lived which would lead to displaced vertices.

subsequently decay purely into jets.

VII.   SIGNALS AT THE LARGE HADRON COLLIDER

We are now ready to study the possible signals of dynamical R-parity conservation at the LHC. For each model, we will outline the final state signals for both the single and pair productions and conduct our analysis on the cross section times branching ratio level only. We will comment on the relevance of the background but of course our comments here would be superseded by a more detailed study of these events.

<u>**Model I**</u>:

As a reminder, we will proceed under the assumption that both the CP-even and CP-odd Higgses decay only into two right-handed neutrinos. This allows for final states consisting of like-sign leptons, an indicator of the Majorana nature of the right-handed neutrinos, as long as the W bosons decay hadronically. In the case were these decays are not possible, the Higgses could decay through off-shell right-handed neutrinos or in a fashion similar to Higgses in Model II depending on the spectrum.

<u>Single Production</u>

$$pp \to X_1 \to N\,N \to e_i^{\pm} W^{\mp} e_j^{\pm} W^{\mp} \to e_i^{\pm} e_j^{\pm} 4j. \tag{69}$$

To get a quick naive estimate for the number of events in this channel we do a back of the envelope calculation using

$$N_{2e4j} \approx \sigma(pp \to X_1) \times \mathrm{BR}(X_1 \to N_1 N_1) \times 2\mathrm{BR}(N_1 \to e^+ W^-)^2 \times \mathrm{BR}(W \to jj)^2 \times \mathcal{L}. \tag{70}$$

Assuming a large luminosity, $\mathcal{L} = 100\ fb^{-1}$, and a large cross section of $10\ fb$ one obtains naively:

$$N_{2e4j} \approx 10 fb \times (1/3) \times 2(3/10)^2 \times (6/9)^2 \times 100 fb^{-1} = 27. \tag{71}$$

Then, indicating that a significant number of events can occur. The exact number of events, $N_{e_n e_m 4j}$, can be calculated taking into account the contributions of all the right-handed neutrinos using the following expression:

$$N_{e_n e_m 4j} = \sigma(pp \to X_1) \times \sum_{a=1\ldots3} \mathrm{BR}(X_1 \to N_a N_a) \times \mathcal{N}_{e_n e_m}^a \times \mathrm{BR}(W \to jj)^2 \times \mathcal{L}, \tag{72}$$

Final State	Combinatorics	Signal	Background
$2\,e^{\pm}\,4\,j$	0.038	62	6
$e^{\pm}\,\mu^{\pm}\,4\,j$	0.030	50	12
$2\,\mu^{\pm}4\,j$	0.027	43	6

TABLE II: Number of events for the three possible two same-sign leptonic final states (with e and μ) for an integrated luminosity of 100 fb^{-1} and a single production cross section of 16.3 fb corresponding to benchmark I with degenerate 95 GeV right-handed neutrinos. We also display the combinatoric factor associated with the branching ratio of the Higgs to right-handed neutrinos, right-handed neutrinos to the specific leptonic final state and W bosons to jets. This factor is independent of the cross section or integrated luminosity and multiplies these two numbers when calculating number of events.

where $\mathcal{N}^a_{e_n e_m}$ is the combinatorical factor for two right-handed neutrinos decaying into $e_n^{\pm} e_m^{\pm}$,

$$\mathcal{N}^a_{e_n e_m} = 2\,\mathrm{BR}(N_a \to e_n^+ W^-) \times \mathrm{BR}(N_a \to e_m^+ W^-) \times \frac{2}{1 + \delta_{nm}}. \qquad (73)$$

We choose a benchmark scenario in order to produce more concrete numbers:

- Benchmark I:

    - $m_{A_{BL}} = 1\,\mathrm{TeV}$, $m_{X_1} = 300\,\mathrm{GeV}$, $m_{Z_{BL}} = 1.5\,\mathrm{TeV}$

    - $m_{\tilde{t}_1} = 150\,\mathrm{GeV}$, all other sfermions at 1 TeV

    - $m_{N_i} = 95\,\mathrm{GeV}$ for $i = 1..3$

    - In this case $\sigma_{pp \to X_1} = 16.3$ fb.

Using these values we display the predicted number of events for the benchmark I in Table II as well as the combinatorical factor associated with the branching ratios of the right-handed neutrinos to charged lepton final states and W to jets. This number is independent of the cross section and integrated luminosity and multiplies both to find the number of events.

Meanwhile, the SM background to this sort of signal has been studied before in Ref. [21], and was found to be dominated by $t\bar{t}W^{\pm}$ production, with a cross section of 4 fb. Using $\mathrm{BR}(t \to j\ell_i^{\pm}\nu) \sim 10\%$, $\mathrm{BR}(W^{\pm} \to \ell_i^{\pm}\nu) \sim 10\%$ and $\mathrm{BR}(t \to jjj) \sim 67\%$ we also include an estimate of the number of background events in Table II. Two important points are worth noting about the background. The first is that the SM background contains missing energy due to the neutrinos [21]. The second and more important is that, as we saw in the last section, the right-handed neutrinos travel a distance of order millimeters before decaying thereby producing displaced vertices, a further powerful handle on the signal over the background. Therefore, using the information about the two displaced vertices in this case one can suppress the SM background. In order to understand the reconstruction of these channels one can use the fact that

the invariant mass of two jets should be equal to M_W, and the invariant mass of two jets and one lepton corresponds to the mass of the right-handed neutrinos [21].

There is also a possible non-SM background from $Z_{BL} \to NN$, also studied in [21], which would of course have the same signal. For masses similar to those in benchmark I, the Z' channel will dominate. Assuming that the Z_{BL} mass is known from the electron or muon channel, the reconstructed mass of the intermediate particle can be used as a handle to differentiate these two channels. For Z_{BL} masses too heavy for the LHC, the single Higgs production might dominate and act as a complimentary discovery channel for this model.

Pair Production

A very important channel is the pair Higgs production through the $B-L$ gauge boson

$$pp \to Z_{BL}^* \to X_1 A_{BL} \to NNNN \to e_i^\pm e_j^\pm e_k^\pm e_l^\pm 8j, \tag{74}$$

because it does not depend directly on supersymmetric particles masses and allows for a more reliable signal for this mechanism stabilizing the LSP without depending on the SUSY spectrum.

We again perform a naive estimate to understand the predictions for the number of events with four same sign leptons and eight jets signal using a cross section of 100 fb and an integrated luminosity of 100 fb^{-1}:

$$
\begin{aligned}
N_{4e8j} &\approx \sigma(pp \to X_1 A_{BL}) \times \mathrm{BR}(X_1 \to N_1 N_1) \times \mathrm{BR}(A_{BL} \to N_1 N_1) \times \\
&\quad 2\mathrm{BR}(N_1 \to e^+ W^-)^4 \times \mathrm{BR}(W \to jj)^4 \times \mathcal{L} \\
&= 100 fb \times (1/3) \times (1/3) \times 2(3/10)^4 \times (6/9)^4 \times 100 fb^{-1} \approx 4. \tag{75}
\end{aligned}
$$

Here we pick a second benchmark scenario:

- Benchmark Scenario II:

    - $m_{A_{BL}} = 220$ GeV, $m_{X_1} = 200$ GeV, $m_{Z_{BL}} = 1$ TeV,

    - $m_{\tilde{t}_1} = 150$ GeV, $m_{\tilde{\tau}_1} = 150$ GeV and all other sfermion at 1 TeV

    - $\mu_{BL} = 150$ GeV, $M_{BL} = 150$ GeV

    - $m_{N_i} = 95$ GeV, for $i = 1..3$.

    - The cross is $\sigma_{pp \to X_1 A_{BL}} = 65.7$ fb.

We display the predicted number of events in Table III for the five possible final states with e and μ leptons. We also show the combinatorics factor which takes into account the branching ratios of the Higgses into

Final State	Combinatorics	Number of Events
$4\,e^{\pm}\,8\,j$	0.00072	4.8
$3\,e^{\pm}\,\mu^{\pm}\,8\,j$	0.0012	7.6
$2\,e^{\pm}\,2\mu^{\pm}\,8\,j$	0.0015	9.7
$e^{\pm}\,3\mu^{\pm}\,8\,j$	0.00081	5.3
$4\mu^{\pm}\,8\,j$	0.00035	2.3

TABLE III: Number of events for the five possible four same-sign leptonic final states for an integrated luminosity of 100 fb^{-1} and a pair production cross section of 65.7 fb corresponding to benchmark II (degenerate 95 GeV right-handed neutrinos). We also display the combinatorics factor which combines the branching ratios for the Higgses into right-handed neutrinos, right-handed neutrinos to specific leptonic final states and W bosons into jets. This factor is independent of the cross section or integrated luminosity and simply multiplies any cross section and integrated luminosity to give the total number of events.

right-handed neutrinos, right-handed neutrinos into leptons and W bosons to jets. This number can be multiplied by the cross section and integrated luminosity to yield the number of events. Note that this second benchmark is in some ways complimentary to benchmark I with respect to the mass of A_{BL}.

In this case the main SM background is $t\bar{t}W^{\pm}t\bar{t}W^{\pm}$ which has a negligible cross section. It is important to mention that in this case one has four displaced vertices making the signal quite special. This does not change the fact though that the reconstruction in this case is quite challenging due to the presence of eight jets in the final state. Imposing the condition that the invariant mass of two jets, $|M(jj) - M_W| < 15$ GeV [21], can improve the reconstruction process as well as the order millimeter displaced vertices due the long lifetimes of the right-handed neutrino. A more detailed study will be considered in a future publication.

<u>Model II</u>:

In this section we assume that $n_{\phi} = 4$ and that the CP-even Higgs S_1, decays into two sfermions while the CP-odd Higgs, A_S decays into S_1 and opposite-sign lepton pairs from an off-shell Z^{*}_{BL} (jets and neutrinos are also possible). Regardless of these concrete assumption, the signals still depends on the SUSY spectrum. We will therefore only highlight some interesting scenarios and finish by addressing some alternatives to the two-body sfermion decays.

- $S_1 \to \tilde{e}\tilde{e}^{*}$: $\tilde{\chi}_1$ as the LSP:

  Here we assume that $m_{\tilde{\chi}_1} < m_{\tilde{e}} < m_{S_1}/2$ and that the lightest neutralino is the LSP (not necessarily a B-L neutralino) and that $\tilde{e}$ is the NLSP.

  Single Production: In the case of the single production one has

  $$pp \to S_1 \to \tilde{e}^{*}\,\tilde{e} \to e^{\pm}e^{\mp}\tilde{\chi}_1\tilde{\chi}_1, \qquad (76)$$

and it yields opposite-sign lepton and missing energy. For benchmark I, where the single production cross section is independent of n_ϕ so that the single production cross section is unchanged ($\sigma_{pp \to S_1} = 16.3$ fb), and the number of events assuming 100% branching ratios and $\mathcal{L} = 1$ fb^{-1} is

$$N_{e^\pm e^\mp E_T^{miss}} = \sigma_{pp \to S_1} \times \text{BR}(S_1 \to \tilde{e}^* \tilde{e}) \times \text{BR}(\tilde{e} \to e\tilde{\chi}_1)^2 \times \mathcal{L} \sim 16. \tag{77}$$

Notice that this estimation is naive because one has to assume a large branching ratio for the decays into selectrons. The main SM background is the WW, ZZ, and $t\bar{t}$ production, but cutting on large missing E_T^{miss} one could reduce this background. See Refs. [33, 34] for recent studies and examples of different techniques.

Pair Production: As we discussed above the pair production can give us a better idea of the cross section without assuming a particular supersymmetric spectrum. In this case one can have the following signals:

$$pp \to S_1 A_S \to \tilde{e}^* \tilde{e} \, S_1 e_i^+ e_i^- \to e^\pm e^\mp e^\pm e^\mp e_i^+ e_i^- \tilde{\chi}_1 \tilde{\chi}_1 \tilde{\chi}_1 \tilde{\chi}_1. \tag{78}$$

Then, in this case one has three pairs of leptons and missing E_T^{miss}. This cross section does depend on the value of n_ϕ, and for benchmark II, $\sigma_{pp \to S_1 A_S} = 160$ fb when $n_\phi = 4$ (note that the Z_{BL} width also changes with n_ϕ so that the cross section doesn't simply scale with this parameter). The number of events for $\mathcal{L} = 1$ fb^{-1} can be estimated as

$$N_{3(e^\pm e^\mp)E_T^{miss}} = \sigma_{pp \to S_1 A_S} \times \text{BR}(Z_{BL} \to e_i^+ e_i^-) \times \mathcal{L} \sim 40, \tag{79}$$

where $\text{BR}(Z_{BL} \to e_i^+ e_i^-) \sim 25\%$ in this case. As in the single production case, demanding a large missing E_T one should be able to reduce the background which is much less severe since it involves more gauge fields or three pairs of top quarks.

- Gravitino LSP and $\tilde{\chi}_1$ NLSP:

  For which we assume the hierarchy: $m_{\tilde{G}} < m_{\tilde{\chi}_1} < m_{\tilde{e}} < m_{S_1}/2$ and that neutralino decays within the detector: $\tilde{\chi}_1 \to \gamma \tilde{G}$.

  Single Production:

$$pp \to S_1 \to \tilde{e}^* \tilde{e} \to e^\pm e^\mp \gamma \gamma \tilde{G} \tilde{G}, \tag{80}$$

is marked by a pair of opposite-sign leptons, photons and missing E_T. The number of events is the same as in the previous scenario since we assuming that all branching ratios are 100%. For benchmark I and $\mathcal{L} = 1 \text{ fb}^{-1}$:

$$N_{e^\pm e^\mp \gamma\gamma E_T^{miss}} = \sigma_{pp \to S_1} \times \mathcal{L} \sim 16. \tag{81}$$

Again, this is a naive estimation of the number of events. It is easy to see that one can satisfy the new bounds from CMS on gauge mediation [35].

Pair Production: One can have channels with multileptons and multiphotons if one uses the Higgs pair production:

$$pp \to S_1 A_S \to \tilde{e}^* \tilde{e} \, S_1 e_i^+ e_i^- \to e^\pm e^\mp e^\pm e^\mp e_i^+ e_i^- \gamma\gamma\gamma\gamma \tilde{G}\tilde{G}\tilde{G}\tilde{G} \tag{82}$$

produces multileptons and multiphotons and missing E_T. The number of events is given by

$$N_{3(e^\pm e^\mp)4\gamma E_T^{miss}} = \sigma_{pp \to S_1 A_{BL}} \times \text{BR}(Z_{BL} \to e_i^+ e_i^-) \times \mathcal{L} \sim 40, \tag{83}$$

for benchmark II, $n_\phi = 4$ and 1 fb^{-1} of integrated luminosity. One can see that these results are in agreement with the bounds from CMS [35].

- $\tilde{\nu}^c$ as the LSP:

  In this case the right-handed sneutrino can be a dark matter candidate and in principle the Higgs S_1 can decay mainly into dark matter, while A_S decays into two leptons and dark matter, $A_S \to S_1 Z_{BL}^* \to S_1 e_i^+ e_i^- \to (\tilde{\nu}^c)^* \tilde{\nu}^c e_i^+ e_i^-$. The number of events can be estimated as in the previous cases. However, since in order to study these channels one needs to make use of the initial state radiation (ISR), we postpone this study for a future publication. For a study on sneutrino dark matter in this context see Ref. [36].

- LSP heavier than S_1:

  Here again there is a lot of variability depending on the specific spectrum. We simply refer the reader to Table IV for the possible final states in this case and leave the calculations for the number of events to a future paper. It is important to mention again that in the case of Model II it is not possible to make well-defined predictions for the signals because we do not know the SUSY spectrum. If one sticks to a particular SUSY breaking scenario one could see which of these signals are the relevant

TABLE IV: Channels with multileptons and multiphotons in Model II when $m_{LSP} > m_{S_1}$.

S_1 Decay	Single production final state	Pair production final state
$S_1 \to \gamma\gamma$	$\gamma\gamma$	$\ell_i^\pm \ell_i^\mp \gamma\gamma\gamma\gamma$
$S_1 \to jj$	jj	$\ell_i^\pm \ell_i^\mp jjjj$
$S_1 \to \ell_j^\pm \ell_j^\mp \ell_k^\pm \ell_k^\mp$	$\ell_j^\pm \ell_j^\mp \ell_k^\pm \ell_k^\mp$	$\ell_i^\pm \ell_i^\mp \ell_j^\pm \ell_j^\mp \ell_k^\pm \ell_k^\mp \ell_l^\pm \ell_l^\mp \ell_m^\pm \ell_m^\mp$

ones. In this paper we pointed out the different possibilities and a detailed study is beyond the scope of this article.

VIII.   SUMMARY

The possibility to test the mechanism responsible for the stability of the lightest supersymmetric particle at the Large Hadron Collider has been investigated in detail. As it has been discussed in this article, the simplest theoretical frameworks where R-parity conservation can be explained dynamically are based on B-L gauge symmetry. We discuss two different models and find the following interesting results:

- In the simplest theoretical frameworks where one can explain dynamically the conservation of R-parity one must have new Higgs bosons which decay mainly into two right-handed neutrinos or into two sfermions.

- We have investigated the production mechanisms and decays of the B-L Higgses. We have found that the Higgs pair production mechanism is quite relevant for the testability of the mechanism for R-parity conservation, because its predictions are independent of the supersymmetric spectrum.

- In Model I, where the B-L Higgs couples at tree level to the right-handed neutrinos, one can have lepton number violating signals with multileptons and multijets. In this case, if the masses of the new Higgses are below 500 GeV one obtains multiple displaced vertices due to the presence of long-lived right-handed neutrinos.

- A new class of models for the dynamical conservation of R-parity has been discussed. In this case the new physical Higgses couple only to the sfermions at tree level and the neutrinos are Dirac fermions. One finds different exotic signals. However, those channels depend on the supersymmetric spectrum. In a simple scenario, such as gauge mediation, one can have channels with multileptons and multiphotons.

The testability of the mechanism for R-parity conservations may help us to understand the link between missing energy at the LHC and the cold dark matter of the universe.

Appendix A: Feynman Rules and Cross Sections

1. Feynman Rules

- Higgs-squark-squark:

$$X_1 \tilde{q}_1^* \tilde{q}_1 : \quad i g^{X_1}_{\tilde{q}_1 \tilde{q}_1} = \frac{i}{6} g_{BL} \, m_{Z_{BL}} \, \sin(\alpha' + \beta') \, \cos 2\theta_{\tilde{q}}, \tag{A1}$$

$$X_1 \tilde{q}_2^* \tilde{q}_2 : \quad i g^{X_1}_{\tilde{q}_2 \tilde{q}_2} = -\frac{i}{6} g_{BL} \, m_{Z_{BL}} \, \sin(\alpha' + \beta') \, \cos 2\theta_{\tilde{q}}, \tag{A2}$$

$$X_1 \tilde{q}_1^* \tilde{q}_2 : \quad i g^{X_1}_{\tilde{q}_1 \tilde{q}_2} = -\frac{i}{6} g_{BL} \, m_{Z_{BL}} \, \sin(\alpha' + \beta') \, \sin 2\theta_{\tilde{q}}, \tag{A3}$$

$$X_2 \tilde{q}_1^* \tilde{q}_1 : \quad i g^{X_2}_{\tilde{q}_1 \tilde{q}_1} = -\frac{i}{6} g_{BL} \, m_{Z_{BL}} \, \cos(\alpha' + \beta') \, \cos 2\theta_{\tilde{q}}, \tag{A4}$$

$$X_2 \tilde{q}_2^* \tilde{q}_2 : \quad i g^{X_2}_{\tilde{q}_2 \tilde{q}_2} = \frac{i}{6} g_{BL} \, m_{Z_{BL}} \, \cos(\alpha' + \beta') \, \cos 2\theta_{\tilde{q}}, \tag{A5}$$

$$X_2 \tilde{q}_1^* \tilde{q}_2 : \quad i g^{X_2}_{\tilde{q}_1 \tilde{q}_2} = \frac{i}{6} g_{BL} \, m_{Z_{BL}} \, \cos(\alpha' + \beta') \, \sin 2\theta_{\tilde{q}}, \tag{A6}$$

for any squark $\tilde{q}$.

- Higgs-fermion-fermion:

$$X_1 N_i N_i : \quad i \, 2\sqrt{2} \, f_i \cos \alpha' = -2 \, i \, g_{BL} \frac{\cos \alpha'}{\sin \beta'} \frac{m_{N_i}}{m_{Z_{BL}}}, \tag{A7}$$

$$X_2 N_i N_i : \quad - i \, 2\sqrt{2} \, f_i \sin \alpha' = 2 \, i \, g_{BL} \frac{\sin \alpha'}{\sin \beta'} \frac{m_{N_i}}{m_{Z_{BL}}}, \tag{A8}$$

$$A_{BL} N_i N_i : \quad 2\sqrt{2} \, f_i \cos \beta' \gamma_5 = -2 \, g_{BL} \frac{1}{\tan \beta'} \frac{m_{N_i}}{m_{Z_{BL}}}, \tag{A9}$$

- quark-squark-gluino:

$$g^{a\mu}\tilde{q}_\alpha^*(p)\tilde{q}_\beta(k): \quad -ig_3(p+k)^\mu \lambda_{\alpha\beta}^a, \tag{A10}$$

$$g^{a\mu}g^{b\nu}\tilde{q}_\alpha^* q_\beta: \quad ig_3^2 \left(\lambda^a\lambda^b + \lambda^b\lambda^a\right)_{\alpha\beta} g^{\mu\nu}, \tag{A11}$$

$$g^{c\mu}\tilde{g}^{b\dagger}\tilde{g}^a: \quad -g_3 f_{abc}\gamma^\mu, \tag{A12}$$

$$q_\alpha \tilde{q}_{1\beta}^* \tilde{g}^a: \quad ig_3\sqrt{2}\lambda_{\alpha\beta}^a \left(\cos\theta_{\tilde{q}} P_L + \sin\theta_{\tilde{q}} P_R\right), \tag{A13}$$

$$q_\alpha \tilde{q}_{2\beta}^* \tilde{g}^a: \quad ig_3\sqrt{2}\lambda_{\alpha\beta}^a \left(-\sin\theta_{\tilde{q}} P_L + \cos\theta_{\tilde{q}} P_R\right), \tag{A14}$$

where λ^a are the generators of $SU(3)$, α and β represent color and f_{abc} are the structure constants for $SU(3)$.

- $Z_{BL}Z_{BL}\phi_i$:

$$Z_{BL}^\mu Z_{BL}^\nu \phi_1: \quad -ig_{BL}n_{BL}m_{Z_{BL}} \sin(\beta' - \alpha')g_{\mu\nu}, \tag{A15}$$

$$Z_{BL}^\mu Z_{BL}^\nu \phi_2: \quad -ig_{BL}n_{BL}m_{Z_{BL}} \cos(\beta' - \alpha')g_{\mu\nu}, \tag{A16}$$

- $Z_{BL}\phi_i A_{BL}$:

$$Z_{BL}^\mu \phi_1 A_{BL}: \quad g_{BL}\frac{n_{BL}}{2}\cos(\alpha' - \beta')(p_1 - p_2)_\mu, \tag{A17}$$

$$Z_{BL}^\mu \phi_2 A_{BL}: \quad g_{BL}\frac{n_{BL}}{2}\sin(\alpha' - \beta')(p_1 - p_2)_\mu, \tag{A18}$$

- $Z_{BL}\bar{f}f$: Here $f = u, d, e$.

$$Z_{BL}^\mu \bar{f}f: \quad -ig_{BL}\frac{n_{BL}^f}{2}\gamma_\mu, \tag{A19}$$

- $Z_{BL}\bar{\nu}\nu$ and $Z_{BL}\bar{N}N$: Here $N = \nu_R + (\nu_R)^C$,

$$Z_{BL}^\mu \bar{\nu}\nu: \quad i\frac{g_{BL}}{2}\gamma_\mu\gamma_5, \tag{A20}$$

$$Z_{BL}^\mu \bar{N}N: \quad i\frac{g_{BL}}{2}\gamma_\mu\gamma_5, \tag{A21}$$

- $Z_{BL}\tilde{f}_i^\dagger \tilde{f}_j$: Here $\tilde{f}_i = \tilde{u}_i^a, \tilde{d}_i^a, \tilde{e}_i^a, \tilde{\nu}_i^a$, where $i, j = 1, 2$ and $a = 1, 2, 3$.

$$Z_{BL}^\mu \tilde{f}_i^\dagger \tilde{f}_j: \quad -i\frac{g_{BL}}{2} n_{BL}^f (p_1 - p_2)_\mu \left(U_{i1}^{\tilde{f}} U_{j1}^{\tilde{f}} + U_{i2}^{\tilde{f}} U_{j2}^{\tilde{f}} \right)^2. \tag{A22}$$

- $Z_{BL}\bar{\chi}_i\chi_j$

$$Z_{BL}^\mu \bar{\chi}_i \chi_j: \quad -i g_{BL} \frac{\eta_{BL}}{2} \left(N_{i\tilde{X}} N_{\tilde{X}j}^\dagger - N_{i\tilde{X}} N_{\tilde{X}j}^\dagger \right) \gamma_\mu \frac{\gamma_5}{2} (1 + \delta_{ij}). \tag{A23}$$

2. Cross Sections

The process $pp \to Z_{BL}^* \to X_1 Z_{BL}$ is described as associated production or Higgs strahlung. The differential partonic cross sections is given by

$$d\hat{\sigma}_{q\bar{q} \to X_1 Z_{BL}}(\hat{s}) = \left| \overline{\mathcal{M}}_{q\bar{q} \to X_1 Z_{BL}}(\hat{s}) \right|^2 \frac{d\mathrm{PS}^{(2)}}{2\hat{s}}, \tag{A24}$$

in terms of the matrix element,

$$\left| \overline{\mathcal{M}}_{q\bar{q} \to X_1 Z_{BL}}(\hat{s}) \right|^2 = \frac{1}{54} \left(\frac{g_{BL}^2 n_{BL}^X}{2} \right)^2 \frac{m_{Z_{BL}}^2 \hat{s} + (\hat{t} - m_{Z_{BL}}^2)(\hat{u} - m_{Z_{BL}}^2)}{(\hat{s} - m_{Z_{BL}}^2)^2 + m_{Z_{BL}}^2 \Gamma_{Z_{BL}}^2} \sin^2 \left(\beta' - \alpha' \right). \tag{A25}$$

The hadronic cross section follows by convolution in analogy to Eq.(53) with the production threshold being $\tau_0 = (m_{X_1} + m_{Z_{BL}})^2/s$.

The result for the Z_{BL} boson fusion, $q(p_1)q'(p_2) \to q(p_3)X_1(p_4)q'(p_5)$, arises from the diagram shown in Fig. 3(d) and the one with crossed external quark lines. In terms of extended Mandelstams, $\hat{t}_{1i} = (p_1 - p_i)^2$ and $\hat{u}_{2i} = (p_2 - p_i)^2$, we can write for the squared matrix element,

$$\left| \overline{\mathcal{M}}_{qq' \to X_1 qq'}(\hat{s}) \right|^2 = \frac{2}{9} \left(\frac{g_{BL}^3 n_{BL}^X}{2} \right)^2 m_{Z_{BL}}^2 \sin^2 \left(\beta' - \alpha' \right)$$

$$\times \left\{ \left[\hat{s}^2 + \hat{s}(\hat{t}_{14} + \hat{u}_{24} - \hat{u}_{23}) - (\hat{t}_{13} + \hat{t}_{14})\hat{u}_{23} + m_{X_1}^2 (\hat{u}_{23} - \hat{s}) \right] \frac{1}{(\hat{u}_{25} - m_{Z_{BL}}^2)^2 (\hat{t}_{13} - m_{Z_{BL}}^2)^2} \right.$$

$$+ \left[\hat{s}^2 + \hat{s}(\hat{u}_{24} + \hat{t}_{14} - \hat{t}_{13}) - (\hat{u}_{23} + \hat{u}_{24})\hat{t}_{13} + m_{X_1}^2 (\hat{t}_{13} - \hat{s}) \right] \frac{1}{(\hat{t}_{15} - m_{Z_{BL}}^2)^2 (\hat{u}_{23} - m_{Z_{BL}}^2)^2} \tag{A26}$$

$$\left. + \left[\frac{3}{2}\hat{s}(\hat{s} + \hat{t}_{14} + \hat{u}_{24} - m_{X_1}^2) \right] \frac{1}{(\hat{u}_{25} - m_{Z_{BL}}^2)(\hat{t}_{15} - m_{Z_{BL}}^2)(\hat{t}_{13} - m_{Z_{BL}}^2)(\hat{u}_{23} - m_{Z_{BL}}^2)}. \right\}$$

The matrix element does not depend on the electric charge or the flavor of the quarks and at the hadronic

level we can just sum over all possible initial states by adding the respective parton densities:

$$d\sigma_{PP \to X_i qq'}(s) = \sum_{q,q'=u,c,d,s} \int_{\tau_0}^1 d\tau \left(\frac{d\mathcal{L}_{qq'}^{PP}}{d\tau} + \frac{d\mathcal{L}_{q\bar{q}'}^{PP}}{d\tau} + \frac{d\mathcal{L}_{\bar{q}\bar{q}'}^{PP}}{d\tau} \right) \left| \overline{\mathcal{M}}_{qq' \to X_1 qq'}(\hat{s}) \right|^2 \frac{1}{2\hat{s}} d\mathrm{PS}^{(3)}, \quad (A27)$$

where $d\mathrm{PS}^{(3)}$ is the 3-particle phase-space element and the production threshold is $\tau_0 = m_{X_1}^2/s$.

[1] M. Drees, R. Godbole and P. Roy, "Theory and Phenomenology of Sparticles," (World Scientific, 2004).

[2] C. S. Aulakh and R. N. Mohapatra, "Neutrino As The Supersymmetric Partner Of The Majoron," Phys. Lett. B **119**, 136 (1982).

[3] M. J. Hayashi and A. Murayama, "Radiative Breaking of $SU(2)_R \times U(1)_{B-L}$ gauge symmetry induced by broken N=1 Supergravity in a Left-Right symmetric model," Phys. Lett. B **153**, 251 (1985).

[4] L. M. Krauss, F. Wilczek, "Discrete Gauge Symmetry in Continuum Theories,' Phys. Rev. Lett. **62**, 1221 (1989); S. P. Martin, "Some simple criteria for gauged R-parity," Phys. Rev. D **46**, 2769 (1992) [arXiv:hep-ph/9207218].

[5] R. Barbier, C. Berat, M. Besancon, M. Chemtob, A. Deandrea, E. Dudas, P. Fayet, S. Lavignac *et al.*, "R-parity violating supersymmetry," Phys. Rept. **420**, 1-202 (2005). [hep-ph/0406039].

[6] P. Nath, P. Fileviez Pérez, "Proton stability in grand unified theories, in strings and in branes," Phys. Rept. **441**, 191-317 (2007). [hep-ph/0601023].

[7] P. Fileviez Pérez, S. Spinner and M. K. Trenkel, "Testing the Mechanism for the LSP Stability at the LHC," arXiv:1103.3824 [hep-ph].

[8] P. Fileviez Pérez, S. Spinner, "Spontaneous R-Parity Breaking and Left-Right Symmetry," Phys. Lett. **B673** (2009) 251-254. [arXiv:0811.3424 [hep-ph]]; V. Barger, P. Fileviez Pérez and S. Spinner, "Minimal gauged $U(1)_{B-L}$ model with spontaneous R-parity violation," Phys. Rev. Lett. **102** (2009) 181802 [arXiv:0812.3661 [hep-ph]].

[9] V. Braun, Y. -H. He, B. A. Ovrut, T. Pantev, "The Exact MSSM spectrum from string theory," JHEP **0605**, 043 (2006). [hep-th/0512177]; M. Ambroso, B. Ovrut, "The B-L/Electroweak Hierarchy in Heterotic String and M-Theory," JHEP **0910**, 011 (2009). [arXiv:0904.4509 [hep-th]].

[10] F. De Campos, O. J. P. Eboli, M. Hirsch, M. B. Magro, W. Porod, D. Restrepo and J. W. F. Valle, "Probing Neutrino Oscillations in Supersymmetric Models at the Large Hadron Collider," Phys. Rev. D **82** (2010) 075002 [arXiv:1006.5075 [hep-ph]].

[11] H. K. Dreiner, S. Grab and T. Stefaniak, "Constraining Selectron LSP Scenarios with Tevatron Trilepton Searches," arXiv:1103.1883 [hep-ph].

[12] P. Bandyopadhyay, P. Ghosh, S. Roy, "An unusual signal of Higgs boson in supersymmetry at the LHC," [arXiv:1012.5762 [hep-ph]].

[13] B. Mukhopadhyaya, S. Mukhopadhyay, "Same-sign trileptons and four-leptons as signatures of new physics at the CERN Large Hadron Collider," Phys. Rev. **D82** (2010) 031501. [arXiv:1005.3051 [hep-ph]].

[14] R. N. Mohapatra, "Mechanism for understanding small neutrino mass in superstring theories," Phys. Rev. Lett. **56**, 561 (1986).

[15] A. Masiero and J. W. F. Valle, "A model for spontaneous R-parity breaking," Phys. Lett. B **251**, 273 (1990).

[16] F. Takayama, M. Yamaguchi, "Gravitino dark matter without R-parity," Phys. Lett. **B485**, 388-392 (2000). [hep-ph/0005214]; W. Buchmuller, L. Covi, K. Hamaguchi, A. Ibarra, T. Yanagida, "Gravitino Dark Matter in R-Parity Breaking Vacua," JHEP **0703**, 037 (2007). [hep-ph/0702184 [HEP-PH]].

[17] P. Langacker, "The Physics of Heavy Z-prime Gauge Bosons," Rev. Mod. Phys. **81** (2009) 1199-1228. [arXiv:0801.1345 [hep-ph]].

[18] L. Basso, A. Belyaev, S. Moretti, G. M. Pruna and C. H. Shepherd-Themistocleous, "Z' discovery potential at the LHC in the minimal $B - L$ extension of the Standard Model," arXiv:1002.3586 [hep-ph].

[19] K. Huitu, S. Khalil, H. Okada, S. K. Rai, "Signatures for right-handed neutrinos at the Large Hadron Collider," Phys. Rev. Lett. **101** (2008) 181802. [arXiv:0803.2799 [hep-ph]].

[20] J. A. Aguilar-Saavedra, "Heavy lepton pair production at LHC: Model discrimination with multi-lepton signals," Nucl. Phys. **B828** (2010) 289-316. [arXiv:0905.2221 [hep-ph]].

[21] P. Fileviez Pérez, T. Han and T. Li, "Testability of Type I Seesaw at the CERN LHC: Revealing the Existence of the B-L Symmetry," Phys. Rev. D **80** (2009) 073015 [arXiv:0907.4186 [hep-ph]].

[22] P. Fileviez Pérez, S. Spinner, "The Fate of R-Parity," Phys. Rev. **D83** (2011) 035004. [arXiv:1005.4930 [hep-ph]].

[23] K. S. Babu, B. Dutta, R. N. Mohapatra, "Lepton flavor violation and the origin of the seesaw mechanism," Phys. Rev. **D67**, 076006 (2003). [hep-ph/0211068].

[24] T. G. Rizzo, "Z' phenomenology and the LHC," [hep-ph/0610104].

[25] P. Minkowski, "Mu → E Gamma At A Rate Of One Out Of 1-Billion Muon Decays?," Phys. Lett. B **67** (1977) 421; T. Yanagida, in *Proceedings of the Workshop on the Unified Theory and the Baryon Number in the Universe*, eds. O. Sawada et al., p. 95, KEK Report 79-18, Tsukuba (1979); M. Gell-Mann, P. Ramond and R. Slansky, in *Supergravity*, eds. P. van Nieuwenhuizen et al., (North-Holland, 1979), p. 315; S.L. Glashow, in *Quarks and Leptons*, Cargèse, eds. M. Lévy et al., (Plenum, 1980), p. 707; R. N. Mohapatra and G. Senjanović, "Neutrino Mass And Spontaneous Parity Nonconservation," Phys. Rev. Lett. **44** (1980) 912.

[26] M. S. Carena, A. Daleo, B. A. Dobrescu and T. M. P. Tait, "Z-prime gauge bosons at the Tevatron," Phys. Rev. D **70** (2004) 093009 [arXiv:hep-ph/0408098].

[27] A. Djouadi, "Squark effects on Higgs boson production and decay at the LHC," Phys. Lett. B **435**, 101 (1998) [arXiv:hep-ph/9806315]; M. Spira, "QCD effects in Higgs physics," Fortsch. Phys. **46**, 203 (1998) [arXiv:hep-ph/9705337].

[28] A. Dabelstein, "Fermionic decays of neutral MSSM Higgs bosons at the one loop level," Nucl. Phys. B **456**, 25 (1995) [arXiv:hep-ph/9503443]; J. A. Coarasa Perez, R. A. Jimenez and J. Sola, "Strong effects on the hadronic widths of the neutral Higgs bosons in the MSSM," Phys. Lett. B **389**, 312 (1996) [arXiv:hep-ph/9511402].

[29] A. D. Martin, W. J. Stirling, R. S. Thorne and G. Watt, "Parton distributions for the LHC," Eur. Phys. J. C **63** (2009) 189 [arXiv:0901.0002 [hep-ph]].

[30] F. del Aguila, J. A. Aguilar-Saavedra, "Distinguishing seesaw models at LHC with multi-lepton signals," Nucl. Phys. **B813**, 22-90 (2009). [arXiv:0808.2468 [hep-ph]].

[31] T. Schwetz, M. Tortola, J. W. F. Valle, "Global neutrino data and recent reactor fluxes: status of three-flavour oscillation parameters," [arXiv:1103.0734 [hep-ph]].

[32] J. A. Casas, A. Ibarra, "Oscillating neutrinos and $\mu \rightarrow e\gamma$," Nucl. Phys. **B618** (2001) 171-204. [hep-ph/0103065].

[33] T. Han, I. -W. Kim, J. Song, "Kinematic Cusps: Determining the Missing Particle Mass at Colliders," Phys. Lett. **B693** (2010) 575-579. [arXiv:0906.5009 [hep-ph]].

[34] A. J. Barr, C. G. Lester, "A Review of the Mass Measurement Techniques proposed for the Large Hadron Collider," J. Phys. G **G37** (2010) 123001. [arXiv:1004.2732 [hep-ph]].

[35] S. Chatrchyan *et al.* [CMS Collaboration], "Search for Supersymmetry in pp Collisions at sqrt(s) = 7 TeV in Events with Two Photons and Missing Transverse Energy," [arXiv:1103.0953 [hep-ex]].

[36] S. Khalil, H. Okada and T. Toma, "Right-handed Sneutrino Dark Matter in Supersymmetric B-L Model," arXiv:1102.4249 [hep-ph].